AGU PUBLICATIONS

Tectonics

RESEARCH ARTICLE
10.1002/2015TC004018

Key Points:
- Central Anatolia formed due to interplay of two simultaneous subduction zones
- The Anatolian thrust belt formed by foreland-propagating nappe stacking
- Strong variations in subduction obliquity may explain contrasting metamorphic histories

Supporting Information:
- Supporting Information S1

Correspondence to:
D. J. J. van Hinsbergen,
d.j.j.vanhinsbergen@uu.nl

Citation:
van Hinsbergen, D. J. J., et al. (2016), Tectonic evolution and paleogeography of the Kırşehir Block and the Central Anatolian Ophiolites, Turkey, *Tectonics*, *35*, 983–1014, doi:10.1002/2015TC004018.

Received 26 AUG 2015
Accepted 15 MAR 2016
Accepted article online 23 MAR 2016
Published online 27 APR 2016

Tectonic evolution and paleogeography of the Kırşehir Block and the Central Anatolian Ophiolites, Turkey

Douwe J. J. van Hinsbergen[1], Marco Maffione[1], Alexis Plunder[1,2], Nuretdin Kaymakcı[3], Morgan Ganerød[4], Bart W. H. Hendriks[4,5], Fernando Corfu[6], Derya Gürer[1], Giovanni I. N. O. de Gelder[1,7], Kalijn Peters[1], Peter J. McPhee[1], Fraukje M. Brouwer[8], Eldert L. Advokaat[1,9], and Reinoud L. M. Vissers[1]

[1]Department of Earth Sciences, University of Utrecht, Utrecht, Netherlands, [2]Université Pierre et Marie Curie, Paris, France, [3]Department of Geological Engineering, Middle East Technical University, Ankara, Turkey, [4]Geological Survey of Norway, Center of Geodynamics, Trondheim, Norway, [5]Statoil ASA, Rotvoll, Norway, [6]Department of Geosciences and Center for Earth Evolution and Dynamics, University of Oslo, Oslo, Norway, [7]Institut de Physique du Globe de Paris, Université Paris Diderot, UMR F-7154 CNRS, Paris, France, [8]Faculty of Earth and Life Sciences, Vrije Universiteit Amsterdam, Amsterdam, Netherlands, [9]SE Asia Research Group, Department of Earth Sciences, Royal Holloway University of London, Egham, United Kingdom

Abstract In Central and Western Anatolia two continent-derived massifs simultaneously underthrusted an oceanic lithosphere in the Cretaceous and ended up with very contrasting metamorphic grades: high pressure, low temperature in the Tavşanlı zone and the low pressure, high temperature in the Kırşehir Block. To assess why, we reconstruct the Cretaceous paleogeography and plate configuration of Central Anatolia using structural, metamorphic, and geochronological constraints and Africa-Europe plate reconstructions. We review and provide new $^{40}Ar/^{39}Ar$ and U/Pb ages from Central Anatolian metamorphic and magmatic rocks and ophiolites and show new paleomagnetic data on the paleo-ridge orientation in a Central Anatolian Ophiolite. Intraoceanic subduction that formed within the Neotethys around 100–90 Ma along connected N-S and E-W striking segments was followed by overriding oceanic plate extension. Already during suprasubduction zone ocean spreading, continental subduction started. We show that the complex geology of central and southern Turkey can at first order be explained by a foreland-propagating thrusting of upper crustal nappes derived from a downgoing, dominantly continental lithosphere: the Kırşehir Block and Tavşanlı zone accreted around 85 Ma, the Afyon zone around 65 Ma, and Taurides accretion continued until after the middle Eocene. We find no argument for Late Cretaceous subduction initiation within a conceptual "Inner Tauride Ocean" between the Kırşehir Block and the Afyon zone as widely inferred. We propose that the major contrast in metamorphic grade between the Kırşehir Block and the Tavşanlı zone primarily results from a major contrast in subduction obliquity and the associated burial rates, higher temperature being reached upon higher subduction obliquity.

1. Introduction

Convergence between the African/Arabian and Eurasian plates since Cretaceous time has formed an intensely deformed and in places metamorphic collage of ophiolitic and continental rocks. Although these have been intensely deformed in a highly noncylindrical fold and thrust belt, the geology of Turkey is at first order what may be expected in a subduction-collision zone: it comprises a thin-skinned fold and thrust belt that in places became subjected to high-pressure, low-temperature blueschist to eclogite facies metamorphism. One striking exception is the Kırşehir Block in the heart of Anatolia, a 200 × 200 × 200 km triangular crystalline massif of continental origin (Figure 1). It contains high-temperature metamorphic rocks and igneous intrusions of Late Cretaceous age. These rocks experienced regional high-grade metamorphism with conditions up to 6–8 kbar and 700–800°C [*Whitney and Dilek*, 2001; *Lefebvre*, 2011; *Lefebvre et al.*, 2015] at much higher temperatures and much lower pressures than recorded by contemporaneous eclogite to blueschist facies continental metamorphic rocks of the Tavşanlı zone (up to 24 kbar and only 500°C) only tens of kilometers to the west [*Sherlock et al.*, 1999; *Davis and Whitney*, 2008; *Whitney et al.*, 2010; *Plunder et al.*, 2013, 2015] (Figure 1). This paper explores a possible explanation for the high geothermal gradient that existed during the Cretaceous metamorphism of the Kırşehir Block.

To this end, we attempt at constraining the plate kinematic context within which the Kırşehir Block metamorphism occurred. Paleogeographic reconstructions invariably suggest that the complex deformation

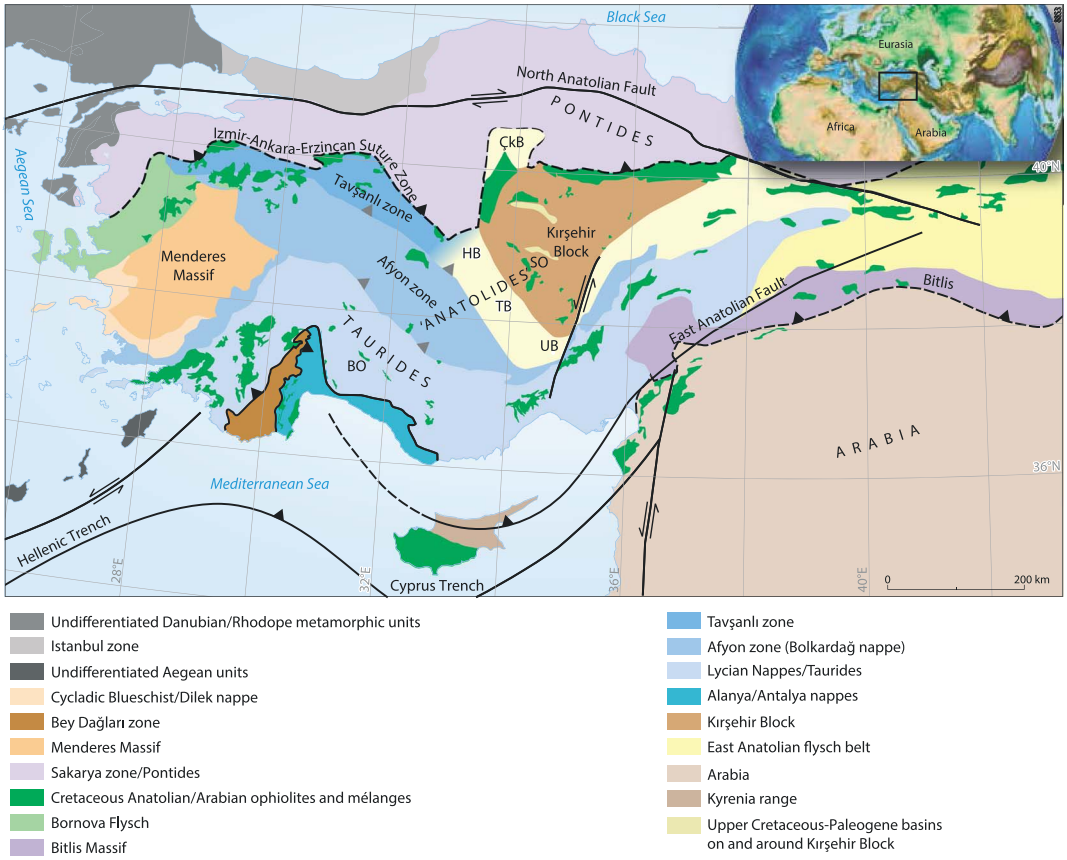

Figure 1. Tectonic map of Turkey, modified after *Advokaat et al.* [2014]. BO = Beyşehir Ophiolite; ÇkB = Çankırı Basin; HB = Haymana Basin, SO = Sarıkaraman ophiolite; TB = Tuzgölü Basin; and UB = Ulukışla Basin.

pattern of Anatolia is caused by subduction of oceanic lithosphere of the Neotethyan Ocean as well as of continental lithosphere of the Anatolide-Tauride fragment that bordered the Neotethys to the south [e.g., *Dewey and Sengör*, 1979; *Sengör and Yilmaz*, 1981; *Okay*, 1986; *Robertson*, 2004; *Barrier and Vrielynck*, 2008; *Moix et al.*, 2008; *Robertson et al.*, 2009; *Pourteau et al.*, 2010; *Lefebvre et al.*, 2013]. These reconstructions show that a minimum of two subduction zones must have existed during the metamorphism of the Tavşanlı zone and the Kırşehir Block. In a northern one, Neotethyan oceanic lithosphere has subducted below the Pontides—the southern Eurasian margin in northern Turkey—since at least Early Cretaceous time [*Okay et al.*, 2006, 2013].

South of the Pontides, the İzmir-Ankara suture zone marks the former subduction zone. To the south lies a fold and thrust belt of ophiolites and Anatolide-Tauride derived units. Detailed studies of these ophiolites have led workers to interpret that at least one more subduction zone must have formed south of the Pontides within the Neotethyan oceanic domain in Late Cretaceous time as attested by widespread circa 95–90 Ma ages of metamorphic soles [*Sengör and Yilmaz*, 1981; *Okay*, 1986; *Robertson*, 2002; *Çelik et al.*, 2006; *Dilek et al.*, 2007; *Aldanmaz et al.*, 2009; *Dilek and Furnes*, 2011; *Parlak et al.*, 2013]. The Anatolide-Tauride units, originally located on the downgoing plate of this intraoceanic subduction zone, were underthrust below and accreted to Neotethyan oceanic lithosphere since Late Cretaceous time [*Sengör and Yilmaz*, 1981; *Robertson et al.*, 2009; *Pourteau et al.*, 2010; *van Hinsbergen et al.*, 2010; *Plunder et al.*, 2013]. Relics of the overriding oceanic lithosphere are preserved as ophiolite klippen that form the highest structural unit above a roof thrust bringing ophiolites in contact with all but the deepest major thrust units of the Anatolide-Taurides. Collision of the Anatolide-Tauride fold and thrust belt and overlying ophiolites with the Pontides formed the Izmir-Ankara suture zone in latest Cretaceous-Paleogene time [*Kaymakci et al.*, 2009; *Meijers et al.*, 2010].

To obtain a first-order kinematic reconstruction of Central Anatolia, we take the following approach: (i) we review structural geological and paleomagnetic constraints on the burial, exhumation, and subsequent deformation history of the Kırşehir Block since Cretaceous time, as well as from ophiolites that overlie the Kırşehir Block; (ii) we assess the plate kinematic context in which the Kırşehir Block as well as the adjacent Tavşanlı zone were buried below the ophiolites and became metamorphosed; (iii) we assess the kinematic history by reviewing the complex geology of Central Turkey and assessing the moment of onset of intra-Neotethyan subduction by reviewing age constraints on the crystallization of ophiolites and the cooling of their metamorphic soles; (iv) we provide new U/Pb ages on plagiogranites of the Sarıkaraman ophiolite that overlies the Kırşehir Block (SO in Figure 1) and determine a paleospreading direction through a paleomagnetic analysis of sheeted dikes of this ophiolite, to be able to take into account in our plate model the orientation of the plate boundary at which the ophiolite formed; (v) we infer the moment of accretion and subsequent exhumation of the metamorphic massifs of Central Anatolia by reviewing geochronological constraints and by adding new U/Pb and $^{40}Ar/^{39}Ar$ ages for rocks of the Kırşehir Block. Together, these constraints define the time window between the onset of intraoceanic subduction and the accretion of the metamorphic domains to the overriding Neotethyan oceanic plate lithosphere represented by the ophiolite klippen; and (vi) we assess the net area loss during this time period from contemporaneous Africa-Europe convergence using Atlantic ocean reconstructions [*Seton et al*., 2012; *Torsvik et al*., 2012]. The combined analysis determines the rate and direction at which the Tavşanlı zone and Kırşehir Block were underthrust and metamorphosed. A possible explanation for the metamorphic contrast between the two domains is offered.

2. Geological Setting

2.1. Cretaceous-Cenozoic Tectonic History of Central Anatolia

Anatolia evolved between the Eurasian and African plates (Figure 1) that have been converging since Early Cretaceous time [e.g., *Torsvik et al*., 2012]. At present, most of Anatolia and the Aegean region can be approximated as a microplate that moves westward relative to Eurasia and Africa/Arabia along the North Anatolian transform fault to the north, the Hellenic and Cyprus trenches in the south, and the East Anatolian fault in the east [e.g., *Reilinger et al*., 2010] (Figure 1). Its plate boundary is diffuse in several places and poorly constrained [e.g., *Biryol et al*., 2011; *van Hinsbergen and Schmid*, 2012; *Özbakır et al*., 2013], and the "microplate" is internally deforming in many places [*Reilinger et al*., 2010; *Koç et al*., 2012, 2016b]. The formation of the microplate is believed to relate to the indentation of Arabia into eastern Anatolia leading to a westward escape [*Dewey and Sengör*, 1979; *Sengör and Kidd*, 1979] and to slab retreat [*Faccenna et al*., 2006; *Sternai et al*., 2014] since the Late Miocene [*Keskin*, 2003; *Sengör et al*., 2003; *Faccenna et al*., 2006; *Hüsing et al*., 2009; *Okay et al*., 2010].

Prior to that time, Anatolia was not a coherent plate, but instead underwent distributed, major internal deformation in the wider Africa-Europe plate boundary zone. At first order, Anatolia is subdivided into two continent-derived fold and thrust belts and an intervening "İzmir-Ankara" suture zone. The Pontide fold and thrust belt in northern Turkey contains rocks that had been part of the southern Eurasian margin since at least the mid-Mesozoic [*Sengör and Yilmaz*, 1981; *Okay and Nikishin*, 2015]. The Anatolide-Tauride domain in central and southern Turkey was derived from continental lithosphere that rifted and drifted away from Gondwana since Triassic time [*Sengör and Yilmaz*, 1981; *Altiner et al*., 1999; *Frizon de Lamotte et al*., 2011] and subsequently became part of the African plate. The Anatolides are comprised of metamorphosed and exhumed massifs in Turkey (Kırşehir Block, Tavşanlı zone, Afyon zone, and Menderes massif; Figure 1) and the Taurides refer to a belt of non-metamorphosed sedimentary rocks (including large platform carbonates) in southern Turkey. The Taurides are a thin-skinned fold and thrust belt formed below ophiolites from Late Cretaceous until at least Eocene time [*Özgül*, 1984], and their Cretaceous nappes are likely the nonmetamorphosed equivalents of some of the metamorphosed "Anatolide" massifs.

One or more Neotethyan oceanic basin(s) once separated the Pontides and Anatolide-Taurides. Relics of this ocean are found offscraped in mélanges, as well as in ophiolites. The oldest known radiolarian cherts found in mélange along the İzmir-Ankara suture have a mid-Triassic age showing a minimum age for the Neotethys Ocean in Turkey [*Tekin et al*., 2002; *Tekin and Göncüoğlu*, 2007]. The ophiolites that are widespread south of the Izmir-Ankara suture have as an added plate kinematic complexity, a suprasubduction zone (SSZ) geochemical signature [*Yalınız et al*., 2000b; *Parlak et al*., 2002; *Dilek et al*., 2007; *Yalınız*, 2008; *Aldanmaz et al*., 2009] suggesting that they formed by spreading above a subduction zone [*Pearce et al*., 1984]. Based on

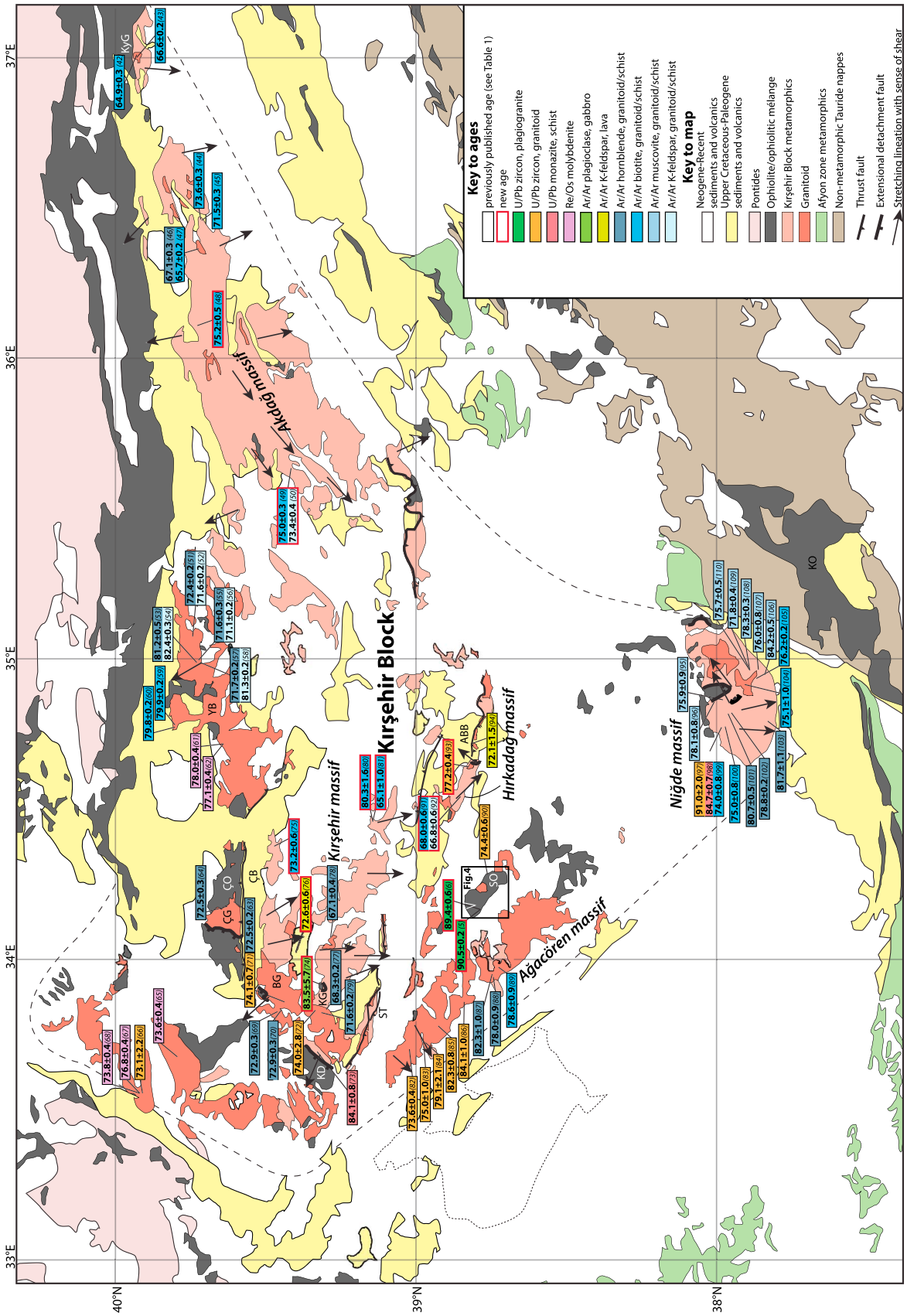

Figure 2. Geological and tectonic map of the Kırşehir Block modified after *MTA* [2002]. Stretching lineation orientations and shear senses are simplified after *Gautier et al.* [2002, 2008], *Işık et al.* [2008], *Işık* [2009], *Lefebvre* [2011], and *Lefebvre et al.* [2011, 2015]. Locations of extensional detachments come from *Gautier et al.* [2008], *Lefebvre* [2011], and *Lefebvre et al.* [2011, 2015]. Locations of thrust faults based on *Köksal and Göncüoglu* [1997], *MTA* [2002], *Yürür and Genç* [2006], *Gülyüz et al.* [2013], *Advokaat et al.* [2014], and *Işık et al.* [2014]. ABB = Ayhan-Büyükkışla Basin; BG = Baranadağ granitoid; ÇB = Çiçekdağı Basin; ÇG = Çiçekdağı Granitoid; ÇO = Çiçekdağı Ophiolite; KD = Kaman Detachment; KG = Kurancalı Gabbro; KO = Karsantı Ophiolite; KyG = Karacayır Granitoid; SO = Sarıkaraman ophiolite; ST = Savcılı Thrust; and YB = Yozgat Batholith. Numbers behind ages refer to listings in Table 1, which also provide the details and references of the ages.

geochemical and metamorphic data SSZ ophiolites are widely interpreted to form shortly (<10 Myr) after subduction initiation [*Casey and Dewey*, 1984; *Stern and Bloomer*, 1992; *Stern et al*., 2012; *Dewey and Casey*, 2013; *Maffione et al*., 2015a; *van Hinsbergen et al*., 2015]. After initiation of subduction, at least one spreading center must therefore have existed within the Neotethyan domain between the subduction zone below the Pontides and the intra-Neotethyan subduction zone(s), close to the intraoceanic trench. This spreading produced oceanic crust, and the amount of lithosphere that subducted in the Anatolian subduction zones in Late Cretaceous time must therefore have been higher than the amount of contemporaneous Africa-Eurasia convergence.

2.2. Upper Cretaceous Crystalline Units

The metamorphic units of western and central Anatolia are subdivided into three massifs based on their metamorphic grade and structural position: the Kırşehir Block in the northeast, the Tavşanlı zone in the northwest, and the Afyon zone fringing both zones to the south (Figure 1).

2.2.1. Kırşehir Block and Central Anatolian Ophiolites

The Kırşehir Block occupies the heart of Anatolia and currently forms a triangular massif also known as the Central Anatolian Crystalline Complex [*Göncüoğlu et al*., 1991; *Lefebvre*, 2011] (Figure 2). It is subdivided into three submassifs, on the basis of common trends of stretching lineations, plutonic belts, and paleomagnetic declinations, bounded by faults: the Akdağ, Kırşehir, and Niğde-Ağaçören-Hırkadağ massifs [*Lefebvre*, 2011; *Lefebvre et al*., 2013] (Figure 2). These are composed of Paleozoic to Mesozoic metasedimentary rocks, intruded by a belt of granitoids [*Kadıoğlu et al*., 2006]. The metamorphic rocks are in places overlain by ultramafic and mafic rocks of an ophiolite suite defined as the Central Anatolian Ophiolites, whereby all elements of the Penrose sequence [*Anonymous*, 1972] can be found. They are, however, severely dismembered and scattered across the Kırşehir Block: ophiolite blocks vary in size from hundreds of meters to tens of kilometers and are only a few hundred meters thick [*Yaliniz et al*., 1996, 2000a, 2000b, 2000c; *Yalınız and Göncüoğlu*, 1998; *Floyd et al*., 2000; *Toksoy-Köksal and Göncüoğlu*, 2001; *Yalınız*, 2008]. It is generally assumed that these ophiolite fragments are the remains of a once coherent oceanic lithosphere below which the Kırşehir Block became underthrust and metamorphosed [*Sengör and Yilmaz*, 1981; *Yaliniz et al*., 1996; *Boztuğ et al*., 2009c]. These ophiolite blocks include well-studied occurrences of ultramafic and mafic bodies such as the Sarıkaraman ophiolite, the Çiçekdağı ophiolite, and the Kurancalı metagabbro (Figure 2). These are the best studied and most complete ophiolitic sequences in the region, and we review their structure and composition to infer the nature and evolution of the lithosphere below which the Kırşehir Block was underthrust.

The most prominent and best studied ophiolite on the Kırşehir Block is the Sarıkaraman ophiolite (Figure 2). It is composed of a crustal sequence of isotropic gabbros intruded by late stage plagiogranites that likely resulted from fractional crystallization of basaltic magmas [*Floyd et al*., 1998; *Yalınız et al*., 2000c; *Toksoy-Köksal et al*., 2001]. This sequence is overlain by sheeted dikes and pillow lavas, plagiogranite-related rhyolites and Turonian-Santonian cherts [*Floyd et al*., 1998; *Yalınız*, 2008]. The ophiolite is intruded by a quartz monzonite pluton that also cuts the underlying high-grade metamorphic rocks of the Kırşehir Block [*Yalınız and Güncüoglu*, 1999; *Yalınız et al*., 1999].

The Çiçekdağı Ophiolite retains a fairly complete crustal sequence with gabbros, dikes, extrusives, and a Turonian-Santonian epi-ophiolitic cover. The Sarıkaraman and Çiçekdağı ophiolites have geochemical compositions consistent with formation at a suprasubduction zone spreading center [*Yaliniz et al*., 1996, 2000a; *Yalınız and Güncüoglu*, 1999]. Mafic blocks in the subophiolitic mélanges, however, have mid-oceanic ridge basalt or, to a lesser degree, ocean island basalt geochemical signatures [*Floyd et al*., 2000] reflecting derivation from the original Neotethyan oceanic crust.

The Kurancalı metagabbro (Figure 2) is a kilometer scale, isolated gabbro body described in detail by *Toksoy-Köksal and Göncüoğlu* [2001] that is interpreted to be a remnant of the severely dismembered Central Anatolian ophiolite sequence [*Yalınız and Göncüoğlu*, 1998; *İlbeyli*, 2008]. It is an isolated body of compositionally layered pyroxene and hornblende gabbro with a calc-alkaline geochemical composition that was interpreted to have formed in an incipient island arc above an intraoceanic subduction zone [*Toksoy-Köksal and Göncüoğlu*, 2001]. The gabbro body measures ~1 km across and is separated from the high-grade metamorphic rocks of the Kırşehir Block by an intensely sheared mélange zone with metaophiolitic and metacarbonate rocks. The gabbros, mélanges, and the Kırşehir Block metamorphic rocks are all intruded by felsic dikes likely related to the nearby Baranadağ granitoid [*Toksoy-Köksal and Göncüoğlu*, 2001] (Figure 2).

The metamorphic rocks of the Kırşehir Block were subjected to regional high-temperature, medium-pressure (HT-MP) conditions and consist of greenschist to upper amphibolite-facies marbles, calcsilicates, metapelites, and quartzites. Peak P-T (Pressure-Temperature) estimates throughout the massif are rather uniform. In the Akdağ massif peak metamorphic conditions were estimated around 5–8 kbar/550–675°C [*Whitney et al*., 2001] and 3.5–6.5 kbar/400–700°C [*Şahin and Erkan*, 1999]. The P-T estimates in the Kırşehir massif reach 6.5–7.5 kbar/700–770°C [*Whitney et al*., 2001]. Parageneses associated with 7–8 kbar/700°C in the Hırkadağ massif are overprinted at 3–4 kbar/800°C during granite intrusion [*Whitney and Dilek*, 2001; *Lefebvre*, 2011; *Lefebvre et al*., 2015]. Analyses of schists of the Niğde massif have yielded metamorphic conditions varying from 5–6 kbar/>700°C to 3–4 kbar/640–650°C, of which the latter conditions likely prevailed during syn-decompressional granitoid intrusion [*Whitney and Dilek*, 1998, 2001]. Similar pressures below 4 kbar were determined for rare schists in the Ağaçören massif close to the granitoid intrusions [*Whitney et al*., 2001]. Regional peak metamorphism hence occurred under conditions up to ~8 kbar/700°C, with local overprints at even higher temperatures up to 800°C but lower pressures of 3–4 kbar during granitoid intrusion. The regional peak metamorphic mineral parageneses are found in a regionally pervasive, flat lying, and mildly undulating foliation [*Seymen*, 1983; *Lefebvre*, 2011].

The regional foliation was cut by a prominent belt of granitoids currently exposed along the western and northern perimeter of the Kırşehir Block [*Yalınız et al*., 1999; *Kadıoğlu et al*., 2003, 2006; *Köksal et al*., 2013] (Figure 2). These granitoids can be subdivided into belts with increasing alkalinity from west to east [*İlbeyli*, 2004a, 2005]. In the Ağaçören massif felsic intrusions occur together with gabbro intrusions that should not be confused with ophiolite-related gabbros [*Kadıoğlu et al*., 2003]. The granitoids' geochemistry shows that they were derived from a mantle source enriched by subduction-related fluids, further contaminated by partial melts of continental crust [*Kadıoğlu et al*., 2003; *İlbeyli*, 2004a, 2005; *İlbeyli et al*., 2009; *Delibaş and Genç*, 2012a; *Köksal et al*., 2013]. Geochemical studies interpreted that melting was triggered by extension of an already hot Kırşehir Block and the decompression of an underlying, metasomatized mantle wedge [*İlbeyli*, 2005; *Köksal et al*., 2013]. Processes such as lithospheric delamination or slab breakoff have been proposed to explain the high temperatures and granitoid intrusions of the Kırşehir Block [*İlbeyli*, 2004a, 2004b, 2005; *Kadıoğlu et al*., 2006; *İlbeyli et al*., 2009; *Köksal et al*., 2012].

The granitoids are largely undeformed, clearly postdating the pervasive regional foliation, and intruded at pressures varying from 2.6 to 5.3 kbar [*İlbeyli*, 2005]. In places, they are deformed by greenschist facies shear zones, interpreted to be syn-exhumational [*Işık et al*., 2008; *Işık*, 2009]. Moreover, the granitoids intrude not only the Kırşehir Block but also the overlying ophiolites and ophiolitic mélange (Figure 2) [e.g., *Yalınız et al*., 1999; *İlbeyli*, 2005]. A detachment fault in marbles near Kaman that accommodated exhumation of the Kırşehir massif relative to anchimetamorphic ophiolitic mélange was intruded by and recrystallized around the Baranadağ granitoid [*Lefebvre et al*., 2011]. These crosscutting relationships show that the Kırşehir Block was buried below oceanic lithosphere represented by the ophiolite remnants and was then intensely deformed and metamorphosed. The block was subsequently intruded by the granitoid belt. These granitoids were affected by and intrude exhumation-related retrograde shear zones. They thus appear to have formed during regional extension and exhumation of the Kırşehir Block [see also *Whitney and Dilek*, 1998; *Whitney et al*., 2003].

Pervasive stretching lineation orientations were mapped in detail by *Lefebvre* [2011] and *Lefebvre et al*. [2011, 2015] for the Akdağ, Kırşehir, and Hırkadağ massifs and by *Gautier et al*. [2008] and *Işık* [2009] for the Niğde and Ağaçören massifs, respectively (Figure 2). The lineations demonstrate that the pervasive regional foliation is associated with a top-to-the-SW sense of shear in the center of the Akdağ massif, a top-to-the-S sense of shear in the center of the Kırşehir massif, and a top-to-the-SSE sense of shear in the center of the Niğde massif. Toward the edges of each massif, however, shear senses in lower grade metamorphic rocks are nearly orthogonal to the syn-regional metamorphic stretching lineations and point from the core of the massifs outward: top-to-the-N in the north and top-to-the-S in the south of the Akdağ massif; top-to-the-NW in the northwest; top-to-the-SE in the southeast of the Kırşehir massif [*Işık et al*., 2008; *Lefebvre*, 2011; *Lefebvre et al*., 2011]; top-to-the-SW in the Ağaçören massif [*Işık*, 2009]; and top-to-the-ENE in the Hırkadağ and Niğde massifs [*Whitney and Dilek*, 2000; *Gautier et al*., 2008; *Lefebvre et al*., 2015]. The lower grade and outward pointing shear senses are in contrast with the main structural trend defined by the Kırşehir Block's granitoid belts and top-to-the-SW lineations that characterize the deeper, central part of the Block and coincide with those on syn-exhumational shear zones and extensional detachments [*Gautier et al*., 2008; *Işık et al*., 2008; *Işık*, 2009; *Lefebvre et al*., 2011, 2015]. They formed during a

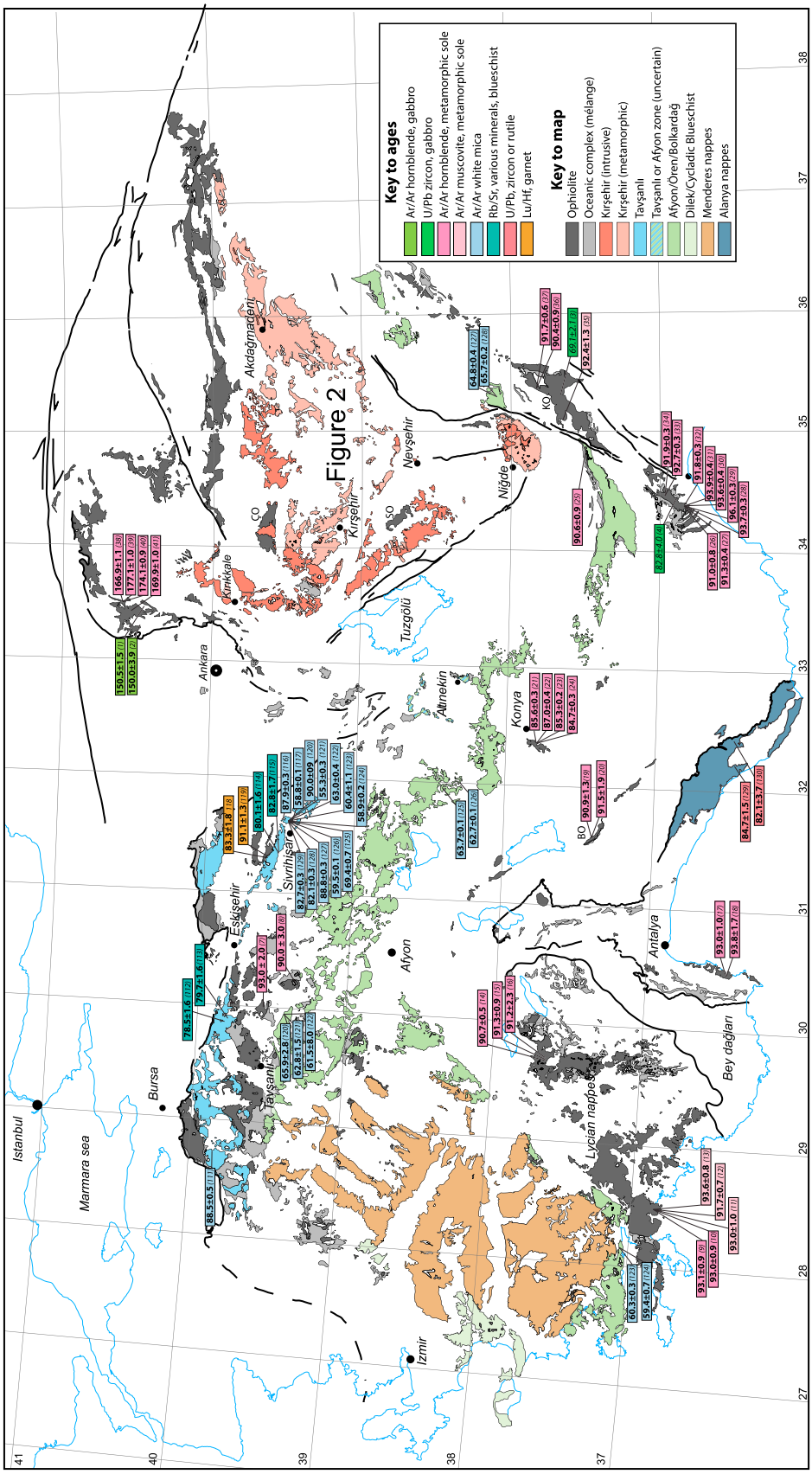

Figure 3. Metamorphic and ophiolite map of Turkey, modified after *MTA* [2002]. Numbers behind ages refer to listings in Table 1. KO = Karsantı Ophiolite.

second phase of deformation postdating formation of the main regional metamorphism and synchronously with granitoid intrusion.

Finally, the Hırkadağ detachment was associated with the formation of the syn-kinematic Ayhan sedimentary basin [*Advokaat et al*., 2014]. In the deepest, syn-extensional part of the stratigraphy a series of upper Cretaceous volcanics yielded a $^{40}Ar/^{39}Ar$ plagioclase age of 72.1 ± 1.5 Ma and extensional faults are unconformably covered by Lutetian limestones [*Advokaat et al*., 2014], which provide the best stratigraphic constraint on the extensional exhumation history of the Kırşehir Block.

2.2.2. Tavşanlı and Afyon Zones

The Tavşanlı zone was defined by *Okay* [1984] and forms an ~EW trending, 300 km long and 50 km wide belt of high-pressure, low-temperature metamorphic rocks. It contains continent-derived metasediments ascribed to the northern margin of the Anatolide-Tauride continent. Tavşanlı rocks were subducted below an oceanic lithosphere in the Cretaceous. Dismembered relics of this lithosphere have been preserved as ophiolites [*Okay and Tüysüz*, 1999; *Okay and Whitney*, 2010]. The Tavşanlı zone sensu stricto is a Paleozoic to Mesozoic sedimentary sequence, composed of detrital sediments at the base grading into platform carbonates. These were metamorphosed under blueschist to eclogite facies conditions, up to 24 kbar/500°C [*Okay*, 2002; *Davis and Whitney*, 2008; *Whitney et al*., 2010; *Plunder et al*., 2013, 2015] during the Late Cretaceous [*Okay and Kelley*, 1994; *Sherlock et al*., 1999; *Sherlock and Kelley*, 2002]. The continental unit that recorded these conditions is also known as the Orhaneli sequence or unit [*Okay*, 1986; *Plunder et al*., 2013].

The Orhaneli sequence is overlain by an accretionary complex, derived from the Neotethyan Ocean. The sequence is mostly made of basalt, tuff, and chert and was divided into three main tectonometamorphic units with increasing metamorphic grade at increasing structural depth from 4–8 kbar/250–300°C to 17 kbar/450°C [*Okay*, 1980a, 1980b, 1982; *Plunder et al*., 2013, 2015]. These ocean-derived units are frequently included in the Tavşanlı zone, but in Figure 3 they are separately indicated, as they do not belong to the passive margin sequence and are also found also atop the Afyon zone. The Tavşanlı and ocean-derived high-pressure units are overlain by ophiolites, and in places they include a metamorphic sole [*Lisenbee*, 1972; *Önen and Hall*, 1993; *Okay et al*., 1998].

To the east, the Tavşanlı zone becomes poorly defined. Blueschist facies continent-derived rocks were reported in numerous places in Anatolia [e.g., *van der Kaaden*, 1966; *Okay*, 1986; *Pourteau et al*., 2010], but these may also be part of the Afyon zone [*van der Kaaden*, 1966; *Okay*, 1986; *Dilek and Whitney*, 1997; *Pourteau et al*., 2010]. The Orhaneli sequence has not been documented to the east or south of the Sivrihisar massif (Figure 3). In the region of Altınekin, blueschist has been described questioning the extent of the Tavşanlı zone [*Droop et al*., 2005]. Most of the rocks described are similar to the oceanic complex described in the Tavşanlı region and share similar P-T conditions at 10.5 kbar/440°C. The HP-LT conditions in the continental rocks of this area at 9.4 kbar/400°C [*Droop et al*., 2005] are identical to some documented in the Afyon zone [*Pourteau et al*., 2014]. Unfortunately, no published data regarding the age of those blueschists are available.

The Afyon zone, part of the Bolkardağ nappe, was originally defined by *Okay* [1984, 1986] as a passive margin sequence metamorphosed under greenschist facies conditions. It is a ~800 km long belt wrapped around the Kırşehir Block to its western, southern, and eastern side (Figure 1). The Afyon zone is overlying the Menderes massif [*Pourteau et al*., 2010]. The Tavşanlı zone structurally overlies the Afyon zone, whereas the exact structural relationships between the Kırşehir Block and the Tavşanlı and Afyon zones cannot be directly observed in the field as they are covered by sedimentary basins. The Tavşanlı and Afyon zones are also structurally overlain by Cretaceous SSZ ophiolites (Figure 3). The discovery of glaucophane in metagabbros of the Pan-African basement units and of Fe-Mg carpholite in conglomerates of the metasedimentary cover interpreted as Permo-Triassic in age constrain the burial history of the Afyon zone with peak pressure-temperature conditions at 10 kbar and 350–400°C [*Rimmelé et al*., 2003; *Candan et al*., 2005; *Pourteau et al*., 2010, 2014].

2.2.3. Post Cretaceous Tectonic History of Central Anatolia

After its exhumation, the Kırşehir Block was broken into three massifs that underwent significant differential vertical axis rotations as shown by paleomagnetic data from Upper Cretaceous granitoids [*Lefebvre et al*., 2013]. Post Lutetian contractional fold and thrust zones with possible strike-slip components accommodated these rotations [*Gülyüz et al*., 2013; *Lefebvre et al*., 2013; *Advokaat et al*., 2014] and remained active until

Table 1. Overview of Available Geochronological Constraints From Anatolian Ophiolites and Their Soles, and the Kırşehir Block, the Tavşanlı and Afyon Zones, and the Alanya Nappes[a]

Number	Sample Code	Rock Type	Mineral	Method	Age (Ma)	Error	Reference
			Ophiolite Crust				
1	FEM 093	gabbro	hornblende	Ar/Ar	150.5	1.5	a
2	FEM 173	gabbro	hornblende	Ar/Ar	150.0	3.9	a
3	FK69	gabbro	zircon	U/Pb	69.1	2.1	b
4	FK57	gabbro	zircon	U/Pb	82.8	4.0	b
5	K27099J	plagiogranite	zircon	U/Pb	90.5	0.2	c
6	K27099C	plagiogranite	zircon	U/Pb	89.4	0.6	c
74	K05107J	gabbro	plagioclase	Ar/Ar	83.5	5.7	c
			Metamorphic Sole				
7	P349	amphibolite	hornblende	Ar/Ar	93.0	2.0	d
8	P534	garnet amphibolite	hornblende	Ar/Ar	90.0	3.0	e
9	YLK-228	amphibolite	hornblende	Ar/Ar	93.1	0.9	f
10	YLK 229	amphibolite	hornblende	Ar/Ar	93.0	0.9	f
11	YLK 253	metamorphic sole schist	muscovite	Ar/Ar	93.0	1.0	f
12	YLK-255	metamorphic sole schist	muscovite	Ar/Ar	91.7	0.7	f
13	YLK266	metamorphic sole schist	muscovite	Ar/Ar	93.6	0.8	f
14	YL-103	amphibolite	hornblende	Ar/Ar	90.7	0.5	f
15	YL-134	amphibolite	hornblende	Ar/Ar	91.3	0.9	f
16	YL-106	amphibolite	hornblende	Ar/Ar	91.2	2.3	f
17	A-292	amphibolite	hornblende	Ar/Ar	93.0	1.0	f
18	A-295	amphibolite	hornblende	Ar/Ar	93.8	1.7	f
19	B-192	amphibolite	hornblende	Ar/Ar	90.9	1.3	f
20	B-194	amphibolite	hornblende	Ar/Ar	91.5	1.9	f
21	A2	amphibolite	hornblende	Ar/Ar	85.6	0.3	g
22	A8	amphibolite	hornblende	Ar/Ar	87.0	0.4	g
23	A12	amphibolite	hornblende	Ar/Ar	85.3	0.2	g
24	A13	amphibolite	hornblende	Ar/Ar	84.7	0.3	g
25	94-PO-65	amphibolite	hornblende	Ar/Ar	90.6	0.9	h
26	93-MO-5	amphibolite	hornblende	Ar/Ar	91.0	0.8	h
27	93-MO-22	amphibolite	hornblende	Ar/Ar	91.3	0.4	h
28	OP 257	amphibolite	hornblende	Ar/Ar	93.7	0.3	j
29	OP 256	amphibolite	hornblende	Ar/Ar	96.1	0.3	j
30	OP 255	amphibolite	hornblende	Ar/Ar	93.6	0.4	j
31	OP 254	amphibolite	hornblende	Ar/Ar	93.9	0.4	j
32	OP 253	amphibolite	hornblende	Ar/Ar	91.8	0.3	j
33	OP 132	amphibolite	hornblende	Ar/Ar	92.7	0.3	j
34	OP 131	amphibolite	hornblende	Ar/Ar	91.9	0.3	j
35	PK-20	metamorphic sole schist	muscovite	Ar/Ar	92.4	1.3	f
36	EY-92-2	amphibolite	hornblende	Ar/Ar	90.4	0.9	h
37	93-AO-3	amphibolite	hornblende	Ar/Ar	91.7	0.6	h
38	FEM-076	amphibolite	hornblende	Ar/Ar	166.9	1.1	k
39	FEM-068	amphibolite	hornblende	Ar/Ar	177.1	1.0	k
40	FEM-067	amphibolite	hornblende	Ar/Ar	174.1	0.9	k
41	FEM-084	amphibolite	hornblende	Ar/Ar	169.9	1.0	k
			Kırşehir Block				
42	BAL 76	syenite	biotite	Ar/Ar	64.9	0.3	l,m
43	BAL 78	syenite	biotite	Ar/Ar	66.6	0.2	l,m
44	BAL 72	leucogranite	biotite	Ar/Ar	73.6	0.3	l
45	BAL 69	leucogranite	biotite	Ar/Ar	71.5	0.3	l
46	BAL 66	granitoid	hornblende	Ar/Ar	67.1	0.3	l
47	BAL 66	granitoid	biotite	Ar/Ar	65.7	0.2	l
48	A22109C	schist	biotite	Ar/Ar	75.2	0.5	c
49	A19109B	schist	biotite	Ar/Ar	75.0	0.3	c
50	A19109B	schist	K-feldspar	Ar/Ar	73.4	0.4	c
51	03 V-34	mylonitized granite	hornblende	Ar/Ar	72.4	0.2	n
52	03 V-34	mylonitized granite	K-feldspar	Ar/Ar	71.6	0.2	n
53	03 V-56	granite	hornblende	Ar/Ar	81.2	0.5	n
54	03 V-56	granite	K-feldspar	Ar/Ar	82.4	0.3	n
55	03 V-47	mylonitized granite	hornblende	Ar/Ar	71.6	0.3	n

Table 1. (continued)

Number	Sample Code	Rock Type	Mineral	Method	Age (Ma)	Error	Reference
56	03 V-47	mylonitized granite	K-feldspar	Ar/Ar	71.1	0.2	n
57	03 V-51	mylonitized granite	hornblende	Ar/Ar	71.7	0.2	n
58	03 V-51	mylonitized granite	K-feldspar	Ar/Ar	81.3	0.2	n
59	BAL 1	leucogranite	biotite	Ar/Ar	79.9	0.2	l
60	BAL 6	leucogranite	biotite	Ar/Ar	79.8	0.2	l
61	BM-2-16B	Mo-Cu deposit	molybdenite	Re/Os	78.0	0.4	o
62	BM-2-11	Mo-Cu deposit	molybdenite	Re/Os	77.1	0.4	o
63	BAL 14	monzogranite	hornblende	Ar/Ar	72.5	0.2	l
64	BAL 13	monzogranite	hornblende	Ar/Ar	72.5	0.3	l
65	BLSH-1	Mo-Cu deposit	molybdenite	Re/Os	73.6	0.4	o
66	LK43	quartz monzonite	zircon	U/Pb	73.1	2.2	p
67	K2-60	Mo-Cu deposit	molybdenite	Re/Os	76.2	0.4	o
68	K3-39	Mo-Cu deposit	molybdenite	Re/Os	73.8	0.4	o
69	BAL 48	quartz syenite	hornblende	Ar/Ar	72.9	0.3	l
70	BAL 47	quartz syenite	hornblende	Ar/Ar	72.9	0.3	l
71	CS	quartz syenite	zircon	U/Pb	74.1	0.7	q
72	BR	quartz monzonite	zircon	U/Pb	74.0	2.8	q
73	KM94-2	migmatitic gneiss	monazite	U/Pb	84.1	0.8	r
75	K21099A	schist	biotite	Ar/Ar	73.2	0.6	c
76	K06108H	rhyolite	K-feldspar	Ar/Ar	72.6	0.6	c
77	BAL 61	quartz monzonite	hornblende	Ar/Ar	68.3	0.2	l, s
78	BAL 34	quartz syenite	hornblende	Ar/Ar	67.1	0.4	l
79	BAL 57	quartz monzonite	hornblende	Ar/Ar	71.6	0.2	l, s
80	K16107A	schist	biotite	Ar/Ar	80.3	1.6	c
81	K18099B	schist	biotite	Ar/Ar	65.1	1.0	c
82	6	monzonite	zircon	U/Pb	73.6	0.4	t
83	5	granite dike	zircon	U/Pb	75.0	1.0	t
84	4	granite dike	zircon	U/Pb	79.1	2.1	t
85	2	granite	zircon	U/Pb	82.3	0.8	t
86	1	granite	zircon	U/Pb	84.1	1.0	t
87	12	gabbro	amphibole	Ar/Ar	82.3	1.0	u
88	10	gabbro	amphibole	Ar/Ar	78.0	0.9	u
89	5	granite	biotite	Ar/Ar	78.6	0.9	u
90	SMS	monzonite	zircon	U/Pb	74.4	0.6	v
91	H191007H	schist	biotite	Ar/Ar	68.0	0.6	c
92	H191007H	schist	K-feldspar	Ar/Ar	66.8	0.6	c
93	H2699C	granitoid	titanite	U/Pb	77.2	0.4	c
94	21-05	andesite	K-feldspar	Ar/Ar	72.1	1.5	w
95	N44	mylonitic gneiss	muscovite	Ar/Ar	75.9	0.9	x
96	N16	granite	muscovite	Ar/Ar	78.1	0.8	x
97	ND98-2	migmatitic gneiss	zircon	U/Pb	91.0	2.0	y
98	ND95-22C	schist	monazite	U/Pb	84.7	0.7	y
99	ND01-30	migmatitic gneiss	biotite	Ar/Ar	74.0	0.8	y
100	N13	granite	biotite	Ar/Ar	75.0	0.8	x
101	ND95-34	schist	hornblende	Ar/Ar	80.7	0.5	y
102	ND01-32	schist	hornblende	Ar/Ar	78.8	0.2	y
103	N8	schist	amphibole	Ar/Ar	81.7	1.1	x
104	N49	granite	biotite	Ar/Ar	75.1	1.0	x
105	ND95-59	migmatitic gneiss	biotite	Ar/Ar	76.2	0.2	y
106	11-TR-03	gneiss	muscovite	Ar/Ar	84.2	0.5	z
107	N67	granite	muscovite	Ar/Ar	76.0	0.8	x
108	11-TR-18	gneiss	muscovite	Ar/Ar	78.2	0.3	z
109	11-TR-17	gneiss	muscovite	Ar/Ar	71.8	0.4	z
110	11-TR-16	gneiss	muscovite	Ar/Ar	75.7	0.5	z
			Tavşanlı Zone				
111	2449	jadeite schist	phengite	Ar/Ar	88.5	0.5	aa
112	96/12	blueschist	multiple	Rb/Sr	78.5	1.6	bb
113	69/198	blueschist	multiple	Rb/Sr	79.7	1.6	bb
114	96/134	blueschist	multiple	Rb/Sr	80.1	1.6	bb
115	96/158	blueschist	multiple	Rb/Sr	82.8	1.7	bb

Table 1. (continued)

Number	Sample Code	Rock Type	Mineral	Method	Age (Ma)	Error	Reference
116	SV02-15	marble	phengite	Ar/Ar	87.9	0.3	cc
117	SV-1-21	marble	muscovite	Ar/Ar	58.8	0.1	cc
118	SV12-01b	blueschist	garnet	Lu/Hf	83.3	1.8	dd
119	SV12-13 F	eclogite	garnet	Lu/Hf	91.1	1.3	dd
120	SV03A29A	quartzite	phengite	Ar/Ar	90.0	0.9	ee
121	SV03-95	quartzite	phengite	Ar/Ar	55.3	0.3	ee
122	SV03A150	quartzite	phengite	Ar/Ar	63.0	0.4	ee
123	SV03A31	quartzite	phengite	Ar/Ar	60.4	1.1	ee
124	SV01-01	marble	phengite	Ar/Ar	58.9	0.2	ee
125	SV02-32C	quartzite	phengite	Ar/Ar	69.4	0.7	ee
126	SV01-21A	quartzite	phengite	Ar/Ar	59.5	0.1	ee
127	SV02-15E	marble	phengite	Ar/Ar	88.8	0.3	ee
128	SV02-08	quartzite	phengite	Ar/Ar	82.1	0.3	ee
129	SV02-18	quartzite	phengite	Ar/Ar	82.7	0.3	ee
			Afyon Zone				
130	Küt0815	carpholite-quartz vein	phengite	Ar/Ar	65.9	2.8	ff
131	Afy0206	phyllite	phengite	Ar/Ar	62.8	1.5	ff
132	Afy0212	phylite	phengite	Ar/Ar	61.5	8.0	ff
133	Ören001	carpholite-quartz vein	phengite	Ar/Ar	60.3	0.3	ff
134	Ören001	carpholite-quartz vein	phengite	Ar/Ar	59.4	0.7	ff
135	OK 4	metarhyolite	phengite	Ar/Ar	63.7	0.1	gg
136	OK 2	metarhyolite	phengite	Ar/Ar	62.7	0.1	gg
137	Yah04	carpholite-quartz vein	phengite	Ar/Ar	64.8	0.4	ff
138	Yah04	carpholite-quartz vein	phengite	Ar/Ar	65.7	0.2	ff
			Alanya Nappes				
139	198/1B	eclogite	zircon	U/Pb	84.7	1.5	hh
140	5/9	eclogite	rutile	U/Pb	82.1	3.7	hh

[a]See Figure 2 for sample locations on the Kırşehir Block and Figure 3 for the locations of all other sample locations. Key to references: a = *Çelik et al.* [2013]; b = *Parlak et al.* [2013]; c = this study, see supporting information; d = *Önen and Hall* [1993]; e = *Önen* [2003]; f = *Çelik et al.* [2006]; g = *Daşçı et al.* [2014]; h = *Dilek et al.* [1999]; j = *Parlak and Delaloye* [1999]; k = *Çelik et al.* [2011]; l = *Boztuğ et al.* [2009c]; m = *Boztuğ et al.* [2009a]; n = *Işık et al.* [2008]; o = *Delibaş and Genç* [2012b]; p = *Delibaş et al.* [2011]; q = *Köksal et al.* [2004]; r = *Whitney and Hamilton* [2004]; s = *Boztuğ et al.* [2009b]; t = *Köksal et al.* [2012]; u = *Kadıoğlu et al.* [2003]; v = *Köksal et al.* [2013]; w = *Advokaat et al.* [2014]; x = *Gautier et al.* [2008]; y = *Whitney et al.* [2003]; z = *Idleman et al.* [2014]; aa = *Okay and Kelley* [1994]; bb = *Sherlock et al.* [1999]; cc = *Seaton et al.* [2009]; dd = *Mulcahy et al.* [2014]; ee = *Seaton et al.* [2014]; ff = *Pourteau et al.* [2013]; gg = *Özdamar et al.* [2013]; and hh = *Cetinkaplan et al.* [2016].

30–20 Ma [*Işık et al.*, 2014]. Indentation of the Kırşehir Block into the Pontides led to formation of a Paleogene northward convex orocline [*Meijers et al.*, 2010] in the center of which N-S contraction inverted Cretaceous normal faults related to the opening of the Black Sea [*Espurt et al.*, 2014]. Contractional deformation in the Çankırı basin in the center of this orocline shows that the northward indentation of the Kırşehir Block lasted until the early Miocene [*Kaymakci et al.*, 2003, 2009].

In the northernmost Kırşehir Block, apatite fission track ages of circa 67–58 Ma were obtained from the Yozgat Batholith, the Çiçekdağı granitoid, and the Karaçayır granitoid [*Boztuğ and Jonckheere*, 2007] (Figure 2). These ages are older than the oldest dated sediments of Lutetian age that unconformably overlie these metamorphic rocks and likely date extensional exhumation of the Kırşehir Block. In the Baranadağ granitoid close to the Kaman Detachment (Figure 2), apatite fission track ages of 47.0 ± 6.2 and 39.2 ± 12.0 Ma [*Fayon et al.*, 2001] are synchronous with the oldest unconformable cover sediments. In the Akdağ massif, apatite fission track ages of 31.6 ± 3.2 and 31.6 ± 3.6 Ma are significantly younger than the oldest sediments that unconformably overlie the metamorphic basement rocks in this area [*Fayon et al.*, 2001] and coincide with and likely relate to late Eocene-Oligocene shortening recorded in sedimentary basins on the Kırşehir Block [*Gülyüz et al.*, 2013; *Advokaat et al.*, 2014]. In the southernmost part of the Kırşehir Block, in the southeastern Niğde massif, very young apatite fission track ages of 11.1 ± 1.8 and 9.4 ± 2.2 Ma were obtained [*Fayon et al.*, 2001], and this part of the massif was interpreted to have been exhumed in the Late Cretaceous, then overthrust and reburied in Oligocene time, and exhumed again in the late Miocene along a top-to-the-SE brittle detachment [*Umhoefer et al.*, 2007; *Whitney et al.*, 2007, 2008; *Idleman et al.*, 2014].

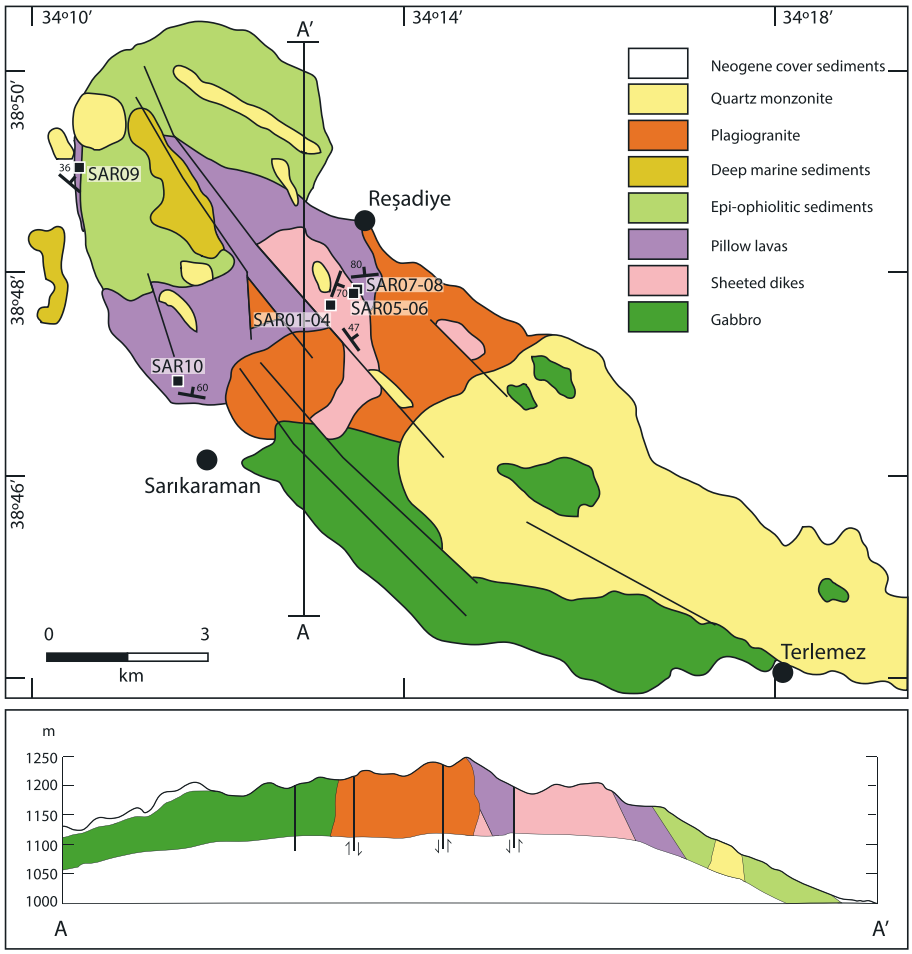

Figure 4. Geological map of the Sarıkaraman ophiolite, modified from *Yaliniz et al*. [1996], with sampling locations. Vertical scale exaggerated.

Simultaneously with the N-S contraction history, western Central Anatolia underwent ~ E-W extension, forming sedimentary basins. The high-grade metamorphic rocks of the Kırşehir Block, which prior to Paleogene rotations formed a N-S elongated body [*Lefebvre et al*., 2013], were exhumed along both top-to-the-east and top-to-the-west extensional shear zones and detachments [*Gautier et al*., 2002, 2008; *Işık et al*., 2008; *Işık*, 2009; *Lefebvre et al*., 2011, 2015]. Eocene and younger extension opened the major NE-SW extensional Tuzgölü basin system in central Anatolia (Figure 1). Up to 8 km of sediments were deposited [*Cemen et al*., 1999; *Aydemir and Ates*, 2006, 2008; *Fernandez-Blanco et al*., 2013] above ophiolites and Upper Cretaceous fore-arc basin sediments, as well as exhumed metamorphic rocks of the Afyon zone [*Görür et al*., 1984]. Middle Miocene to presently active multidirectional (E-W and N-S) extension has controlled the formation of basins farther to the west, on top of the Central Taurides [*Koç et al*., 2012, 2016b]. The area between the Taurides and Pontides was thus much wider than today in a N-S direction, and at the onset of the Cenozoic the distance between the Central Taurides and the Kırşehir Block in an E-W direction was likely considerably narrower than today.

3. Review of Geochronological Constraints on Central Anatolian Ophiolites and Magmatic and Metamorphic Rocks

In this section, we review published $^{40}Ar/^{39}Ar$, U/Pb, Lu/Hf, and Re/Os ages of Central Anatolia, details of which are provided in Figures 2 and 3 and Table 1. We include all ages obtained with these techniques from the ophiolites south of the İzmir-Ankara suture, the metamorphic rocks of the Tavşanlı and Afyon zones, and the metamorphic and igneous rocks of the Kırşehir Block and overlying volcanics. This compilation includes

AGU Tectonics

10.1002/2015TC004018

Table 2. U/Pb Data

Sample[a]	Weight (ug)	U[b] (ppm)	Th/U[c]	Pbc[d] (pg)	$^{206}Pb/^{204}Pb$[e]	$^{207}Pb/^{235}U$[f]	± 2 s (abs)	$^{206}Pb/^{238}U$[f]	± 2 s (abs)	Rho	$^{207}Pb/^{206}Pb$[f]	± 2 s (abs)	$^{206}Pb/^{238}U$[f] (Age in Ma)	± 2 s	$^{207}Pb/^{235}U$[f] (Age in Ma)	± 2 s
C-10-3 = K27099J, Plagiogranite, Eastern Part of Sarikaraman Massif																
Z eu sp CA [20]	23	73	0.41	16.7	109	0.0992	0.0035	0.014431	0.000065	0.18	0.0498	0.0017	92.36	0.41	96.02	3.19
Z fr CA [>20]	31	57	0.42	1.4	1166	0.0947	0.0007	0.014241	0.000038	0.52	0.0482	0.0003	91.15	0.24	91.89	0.69
Z eu-an sp CA [19]	25	71	0.41	1.8	876	0.0931	0.0010	0.014159	0.000053	0.51	0.0477	0.0004	90.63	0.34	90.39	0.89
Z an sp CA [19]	24	88	0.66	4.7	414	0.0941	0.0010	0.014157	0.000035	0.47	0.0482	0.0005	90.62	0.22	91.31	0.96
Z fr CA [>20]	17	69	0.44	1.4	750	0.0930	0.0010	0.014132	0.000036	0.47	0.0477	0.0005	90.46	0.23	90.25	0.95
C-10-2c = K27099C, Plagiogranite, Sarikaraman Ophiolite																
Z eu sp CA [1]	13	28	0.19	5.7	76	0.0983	0.0061	0.014303	0.000088	0.39	0.0498	0.0030	91.55	0.56	95.21	5.60
Z eu sp CA [10]	13	160	0.60	4.7	412	0.0944	0.0011	0.014104	0.000038	0.47	0.0485	0.0005	90.28	0.24	91.56	0.99
Z eu sp fr CA [17]	35	190	0.32	2.3	2492	0.0926	0.0004	0.013974	0.000035	0.70	0.0481	0.0002	89.46	0.22	89.92	0.40
Z eu sp AA [17]	40	152	0.47	6.3	859	0.0929	0.0006	0.013965	0.000035	0.59	0.0482	0.0002	89.40	0.22	90.18	0.51
Z eu-an sp CA [5]	81	39	0.45	8.0	361	0.0925	0.0010	0.013971	0.000037	0.42	0.0480	0.0005	89.44	0.23	89.83	0.97
Z fr pbr AA [4]	54	225	0.46	8.8	1212	0.0921	0.0004	0.013896	0.000032	0.62	0.0481	0.0002	88.96	0.20	89.44	0.37

[a] Z = zircon; T = titanite; eu = euhedral; an = anhedral; sp = short prismatic; fr = fragments; pbr = pale brown; br = brown; tu = turbid; AA = air abrasion; CA = chemical abrasion; NA = not abraded; and [1] = number of grains.
[b] U concentration know to about 10%, except for weight at or below 1 μg.
[c] Th/U model ratio inferred from 208/206 ratio and age of sample.
[d] Total amount of common Pb (initial + blank).
[e] Raw data corrected for fractionation.
[f] Corrected for fractionation, spike, blank and initial common Pb; error calculated by propagating the main sources of uncertainty; the initial common Pb of zircon corrected using *Stacey and Kramers* [1975] model compositions; the initial common Pb of titanite corrected using the composition of lead in coexisting amphibole: $^{206}Pb/^{204}Pb = 18.617$ (±0.030), $^{207}Pb/^{204}Pb = 15.717$ (±0.030); $^{206}Pb/^{238}U$ and $^{207}Pb/^{206}Pb$ values corrected for excess ^{206}Pb assuming Th/U = 4 for the parental magma and using the equation of *Schärer* [1984].

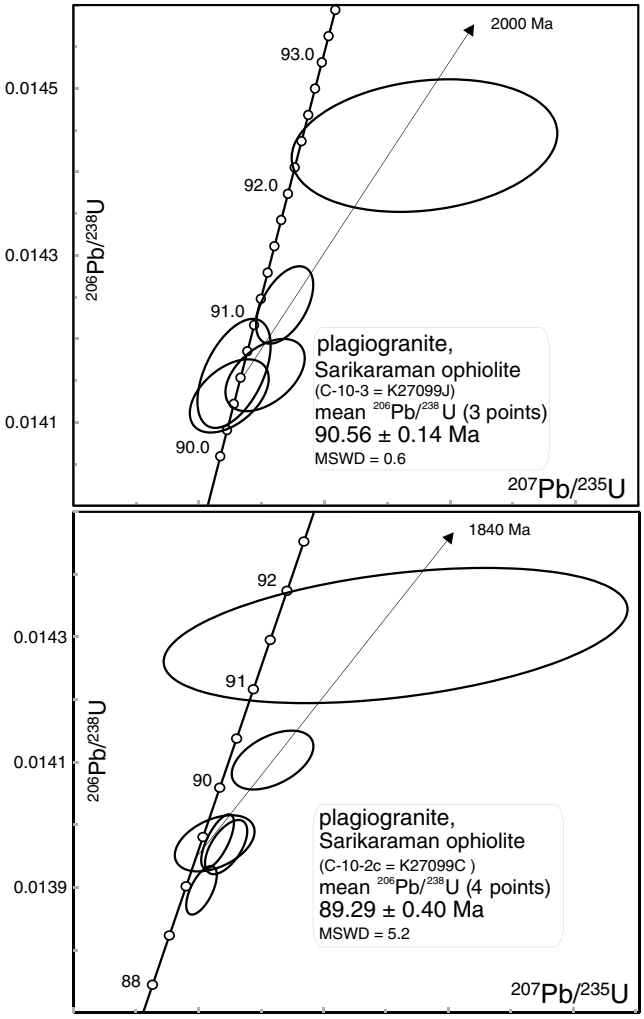

Figure 5. Concordia diagram displaying zircon U-Pb data from plagiogranites of the Sarıkaraman ophiolite. Ellipses indicate the 2σ uncertainty.

previously unpublished $^{40}Ar/^{39}Ar$ and U/Pb ages mentioned in the PhD thesis of *Lefebvre* [2011]. Technical details of these analyses are given in the online Appendix A.

Metamorphism in the Menderes massif is Cenozoic and Precambrian in age [*Oberhänsli et al*., 1997; *Gessner et al*., 2004; *Candan et al*., 2015] and is not included in further detail in the overview in Figure 3. We focus our review on high-precision analytical techniques and for that reason (Figures 2 and 3) we have not incorporated K-Ar ages, such as those from metamorphic soles of *Çelik* [2008]. We note that those ages generally cluster in the same age range: K-Ar ages from the Afyon zone of *Özdamar et al*. [2012] are similar to $^{40}Ar/^{39}Ar$ ages of 60–65 Ma reported by the same authors [*Özdamar et al*., 2013]. The first radiometric age constraints for the metamorphism and magmatism of the Kırşehir Block were also derived from K-Ar and Rb-Sr dating techniques on whole-rock samples or mineral separates [e.g., *Göncüoğlu*, 1986; *Zeck and Ünlü*, 1988; *Güleç*, 1994; *Yalınız et al*., 1999; *İlbeyli*, 2004a; *Tatar and Boztuğ*, 2005; *Boztuğ and Harlavan*, 2007]. These ages, interpreted to reflect granitoid intrusion and/or cooling of the Kırşehir Block during exhumation, are generally in the same ranges as the more modern, higher precision $^{40}Ar/^{39}Ar$ and U/Pb ages that are compiled in Table 1 and Figure 2. They show intrusion and cooling ages in the circa 85–65 Ma range, but also include some outliers, particularly toward older ages (110 ± 5 and 110 ± 14 Ma Rb/Sr whole rock granitoid ages [*Zeck and Ünlü*, 1988; *Güleç*, 1994]), which have not been confirmed by more modern techniques.

We also do not take into account a series of $^{207}Pb/^{206}Pb$ single zircon evaporation ages from granitoids of the Kırşehir Block that were reported by *Boztuğ et al*. [2007], ranging from 99.0 ± 11.0 Ma to 74.1 ± 4.9 Ma. These ages are mostly within error of the U/Pb ages obtained from the same granite bodies summarized in Table 1 and Figure 2. Three ages of 95.7 ± 5.1 Ma, 97.0 ± 12.0 Ma, and 99.0 ± 11.0 Ma were reported by *Boztuğ et al*. [2007] from granitoids cutting the syn-regional metamorphism foliation. These are significantly older than U/Pb monazite ages of a migmatite from the Kırşehir massif and a sillimanite schist from the Niğde massif that were deformed by the regional foliation around 84.1 ± 0.8 Ma and 84.7 ± 0.7 Ma [*Whitney et al*., 2003; *Whitney and Hamilton*, 2004]. These $^{207}Pb/^{206}Pb$ ages violate crosscutting relationships, and given their large error bars and the lack of corroboration by higher precision U/Pb zircon dating techniques, we disregard these age results.

4. Sarıkaraman Ophiolite

To include the formation of the Central Anatolian Ophiolites in the plate tectonic context we here provide new data on the age and paleospreading direction of the ridge at which the Sarıkaraman ophiolite formed (Figure 4).

Table 3. Paleomagnetic Results From the Sarıkaraman Ophiolite[a]

Site	Lithology	Latitude	Longitude	Strike/Dip	N	N_{45}	D_{GEO}	dD_{GEO}	I_{GEO}	dI_{GEO}	D_{TC}	I_{TC}	k	α_{95}	K	A_{95}	A_{95min}	A_{95max}
SAR01	Sheeted dikes	38°47′18.5″	34°12′40.8″	324/47	8	5	006.1	28.9	58.7	19.9	-	-	20.2	17.4	13.1	21.9	6.3	29.7
SAR02	Sheeted dikes	38°47′15.9″	34°12′43.8″	324/47	3	3	352.5	24.1	42.5	28.7	-	-	30.4	22.7	33.0	21.8	7.7	41.0
SAR03	Sheeted dikes	38°47′42.2″	34°12′33.5″	324/47	6	5	349.9	17.8	46.8	18.9	-	-	17.1	19.1	24.7	19.1	6.3	29.7
SAR01-02-03	Sheeted dikes	-	-	324/47	17	13	355.7	12.1	50.6	11.4	-	-	19.2	9.7	17.0	10.3	4.3	16.3
SAR04	Sheeted dikes	38°47′18.5″	34°12′43.8″	326/86	14	14	260.9	78.3	83.3	6.7	-	-	34.1	6.9	10.5	12.9	4.2	15.6
SAR05	Sheeted dikes	38°47′17.4″	34°12′55.4″	020/70	10	7	042.0	18.1	32.3	27.1	-	-	13.2	19.4	13.2	17.2	5.5	24.1
SAR06	Sheeted dikes	38°47′18.3″	34°12′51.5″	020/70	10	10	266.5	14.2	18.4	26.0	-	-	8.3	17.9	12.8	14.0	4.8	19.2
SAR07	Pillow lavas	38°47′19.7″	34°12′53.4″	264/80	13	11	208.1	19.3	61.2	12.0	335.2	33.0	21.7	10.0	11.4	14.2	4.6	18.1
SAR08	Pillow lavas	38°47′18.6″	34°12′57.8″	264/80	24	21	198.4	16.4	67.7	7.4	343.6	30.1	21.3	7.0	10.5	10.3	3.6	12.0
SAR09	Pillow lavas	38°48′40.3″	34°10′27.2″	310/36	22	21	321.9	11.5	60.1	7.5	000.5	39.9	27.2	6.2	14.6	8.6	3.6	12.0
SAR10	Pillow lavas	38°46′39.5″	34°11′26.1″	280/60	7	4	317.9	36.6	64.5	18.9	349.6	12.8	31.9	16.5	15.2	24.3	6.9	34.2
SAR07-08-09-10	Pillow lavas	-	-	-	57	57	-	-	-	-	348.4	33.2	18.2	4.6	20.6	4.3	2.4	6.5

[a]Local structural attitude is expressed as azimuth/plunge. N, number of samples analyzed per site. N_{45}, number of samples used form the computation of the site mean value after applying a fixed 45° cutoff to the data set [*Johnson et al.*, 2008]. D_{GEO} and I_{GEO}, in situ site mean declination and inclination. D_{TC} and I_{TC}, tilt-corrected site mean declination and inclination for the volcanic sequence only. dDis and dIis, error associated to the in situ declination and inclination. k and α_{95}, precision parameter and semiangle of the 95% cone of confidence around the mean value for the characteristic remanent magnetization (ChRM) distribution, after *Fisher* [1953]. K and A_{95}, precision parameter and semiangle of the 95% cone of confidence around the mean value for the virtual geomagnetic poles (VGP) associated to the relative ChRMs. A_{95max} and A_{95min}, maximum and minimum value of A_{95} expected from paleosecular variation of the geomagnetic field, after *Deenen et al.* [2011].

To this end, we dated two samples from plagiogranite dikes in gabbros of the ophiolite and provide a paleomagnetic analysis of pillow lavas and sheeted dikes of the ophiolite.

4.1. U/Pb Geochronology

Two samples were collected for U/Pb analysis from plagiogranite intrusions in the Sarıkaraman ophiolite (K27099C and K27099J) (Figure 4). Zircons were extracted by crushing and pulverizing the samples followed by concentration of the heavy minerals with a Wilfley table, heavy liquids, and magnetic separators. The grains were then selected under a binocular microscope and subjected to either air abrasion [*Krogh*, 1982] or chemical abrasion [*Mattinson*, 2005]. The chosen grains were analyzed by ID-TIMS following the procedure of *Krogh* [1973] with modifications described in *Corfu* [2004] and with the use of a mixed ^{202}Pb-^{205}Pb-^{235}U spike. Decay constants are those of *Jaffey et al.* [1971] and the U composition used was ^{238}U/^{235}U = 137.88. The data are corrected for blanks of 2 pg Pb and 0.1 pg U and for ^{230}Th disequilibrium [*Schärer*, 1984] (Table 2). Plotting and age calculation was done with the program Isoplot [*Ludwig*, 2003] (Figure 5).

Sample K27099J comprised mainly short prismatic zircon crystals with some morphological variations. The five analyses comprise two discordant data points, which reflect an inherited Paleoproterozoic component, and three overlapping concordant analyses giving an average ^{206}Pb/^{238}U age of 90.56 ± 0.14 Ma. This age is interpreted as the time of crystallization of the plagiogranite.

Sample K27099C also contained some xenocrystic zircon components of Paleoproterozoic origin (Figure 5) in a population of euhedral zircon crystals and fragments. Three of the analyses overlap the Concordia curve defining an average ^{206}Pb/^{238}U age of 89.43 ± 0.13 Ma. Another analysis is slightly younger, either because of some Pb loss, or because the three concordant analyses all have tiny amounts of older Pb. These geological uncertainties are included in the larger error of the average of 89.29 ± 0.40 Ma calculated from all four analyses. The latter age is preferred as the more conservative estimate of the time of emplacement of the plagiogranite.

4.2. Paleomagnetism

4.2.1. Sampling and Methods

Sheeted dike complexes form by repeated injection of magma along vertical fractures at an

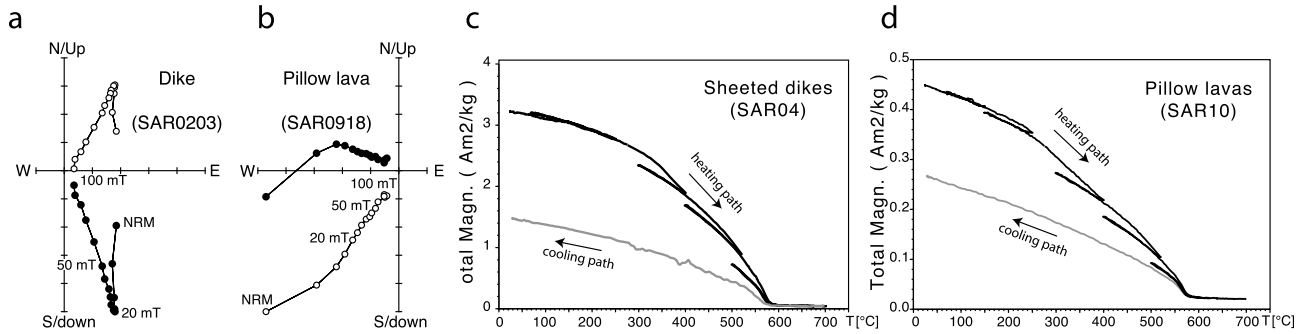

Figure 6. Orthogonal vector plots [*Zijderveld*, 1967] of representative samples (in situ coordinates) from (a) the sheeted dike complex and (b) the pillow basalts. Solid and open dots represent projections on the horizontal and vertical planes, respectively. Demagnetization step values in mT are shown. (c, d) Results from the Curie balance experiments for two representative specimens from the sheeted dikes and pillow basalts.

oceanic spreading center and are therefore parallel to it. For many years geologists have used the sheeted dikes in ophiolites to reconstruct the orientation the spreading ridge and from this the paleospreading directions [*Nicolas et al*., 1988; *Morris et al*., 1998; *Nicolas et al*., 2000; *Maffione et al*., 2015a]. However, it has been demonstrated that using the strike of the dikes alone can produce critical errors in the estimate of the spreading directions [*Kirker and McClelland*, 1996]. A better approach requires the use of both structural geological and paleomagnetic constraints.

To this aim, paleomagnetic samples were collected from doleritic sheeted dikes (six sites and 51 samples) and pillow basalts (four sites and 66 samples) within the Sarıkaraman ophiolite (Table 3 and Figure 4) to determine the paleospreading direction of the Sarıkaraman ophiolite around the time of crystallization of the plagiogranites dated in the previous section. Pillow basalts are relatively abundant and well preserved in the sampling area, while sheeted dikes are scarce. Dikes were sampled only where clear chilled margins were identified so that their orientations could be conclusively determined. Layering of the pillow basalts could be clearly identified in the field, also thanks to local occurrence of radiolarian cherts (Site SAR09) overlying the basalts. Both dikes and lavas are affected by seafloor low-temperature greenschist facies metamorphism associated to hydrothermal alteration at the spreading ridge.

Magnetic remanence was analyzed with a stepwise alternating field demagnetization treatment using a robotized cryogenic magnetometer (2G Enterprises) installed in the paleomagnetic laboratory "Fort Hoofddijk" (Utrecht University). Remanence components were isolated via principal component analysis [*Kirschvink*, 1980] using Remasoft 3.0 software [*Chadima and Hrouda*, 2006]. Site mean paleomagnetic directions were calculated using a Fisherian [*Fisher*, 1953] statistics on virtual geomagnetic poles (VGPs) after applying a fixed 45° cutoff [*Johnson et al*., 2008]. Variation of the magnetic remanence during stepwise heating-cooling cycles was measured in representative samples using a modified horizontal translation Curie balance [*Mullender et al*., 1993] to identify the nature of the magnetic carriers.

4.2.2. Net Tectonic Rotation Analysis

In sheeted dike complexes where paleohorizontal constraints are commonly absent, as well as in regions affected by multiple phases of deformations, a net tectonic rotation approach [*Allerton and Vine*, 1987] has been demonstrated to be a more suitable and reliable method to investigate tectonic rotations using paleomagnetic constraints [*Morris et al*., 1990; *Hurst et al*., 1992; *Morris et al*., 1998; *Inwood et al*., 2009; *Maffione et al*., 2015a]. The robustness of this analysis lies in the fact that rocks are not just restored to their predeformation orientation (i.e., vertical for dikes) as in classical paleomagnetic approach but also their in situ paleomagnetic directions are restored parallel to the expected predeformation directions (i.e., the reference direction). Independently from the number of tectonic phases that occurred, net tectonic rotation analysis can calculate the direction of the rotation axis and the amount and sense of the rotation responsible for the (net) deformation and restores the rock units to their original (predeformation) orientation.

4.2.3. Results

High-stability characteristic remanent magnetizations (ChRMs) were effectively isolated in all samples between 20 and 100 mT (Figures 6a and 6b), excluding the occurrence of secondary high-coercivity magnetic phases like iron sulphides or hematite. Curie temperatures of 560–570°C determined from the Curie balance experiments (Figures 6c and 6d) confirmed that the main magnetic carriers are low-coercivity

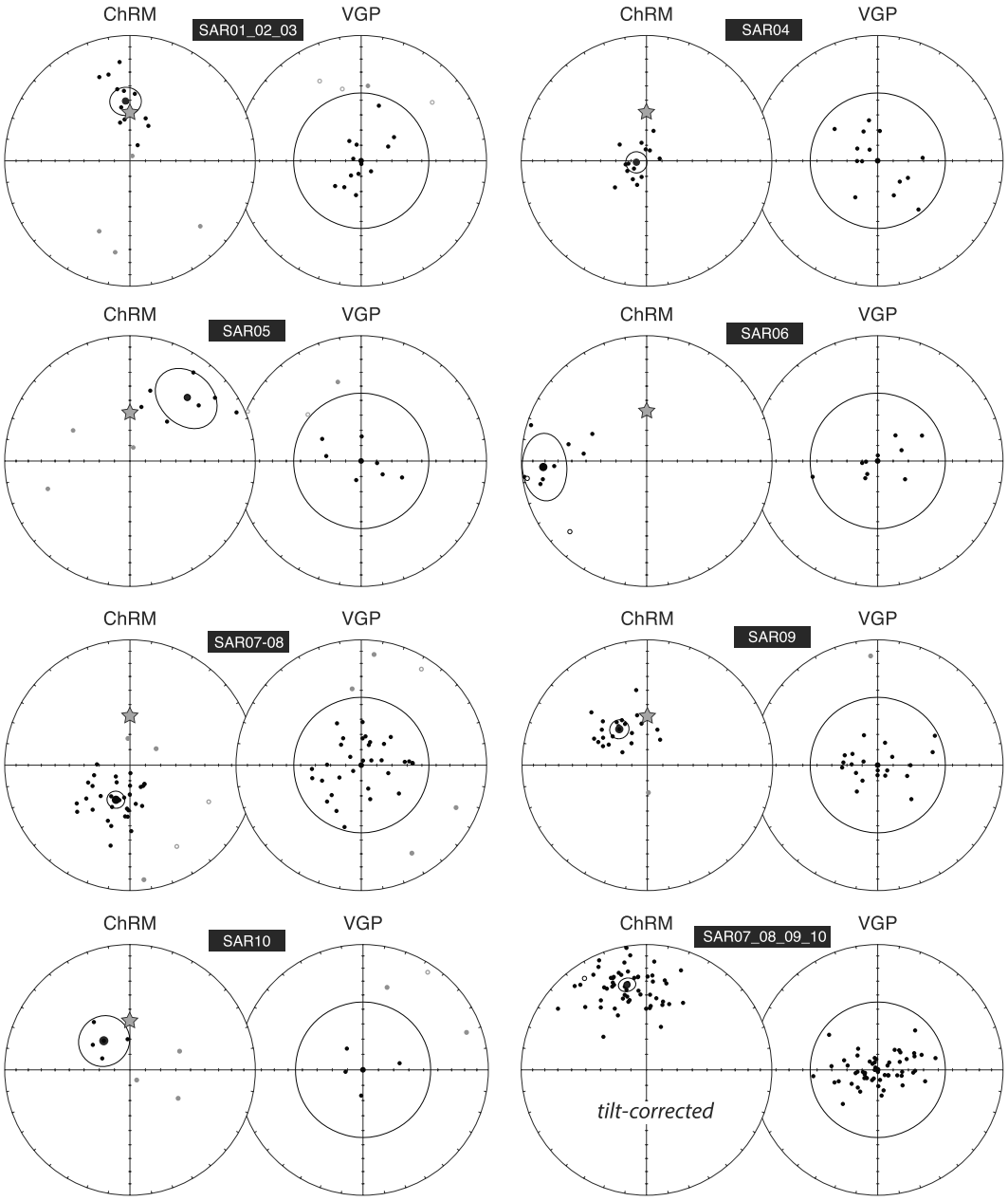

Figure 7. Stereographic projection (lower hemisphere) of the in situ characteristic remanent magnetizations (ChRMs) and correspondent virtual geomagnetic poles (VGPs) for the sampled sites. Site mean remanence directions (large black dots) and associated 95% cones of confidence around them (ellipses) are shown. Solid/open dots correspond to normal/reversed magnetic polarity. Grey star indicates the direction of the present-day geomagnetic field ($D/I = 000°/58.1°$) at the sampling locality. Grey dots are the direction discarded after filtering with a 45° cutoff (circle in the VGP plots).

nearly pure magnetite grains. Curie temperatures ranging from ~350°C to 560°C were also observed, suggesting minor occurrence of high-Ti titanomagnetite [*Dunlop and Özdemir*, 1997].

The ChRMs/VGP scatter is consistent with a typical paleosecular variation-induced scatter ($A_{95min} < A_{95} < A_{95max}$; sensu *Deenen et al.* [2011]) (Table 3 and Figure 7). This supports a primary (pre-tilt) origin of the remanence, and making both remagnetization (resulting in $A_{95} < A_{95min}$) and high-internal rotations (resulting in $A_{95} > A_{95max}$) unlikely. A recent remagnetization of the studied rocks can also be excluded because the in situ site mean directions are substantially different from the present-day field at the sampling locality (declination/inclination = 000°/58°; Figure 7). Based on this evidence, we consider the magnetization of the studied rocks

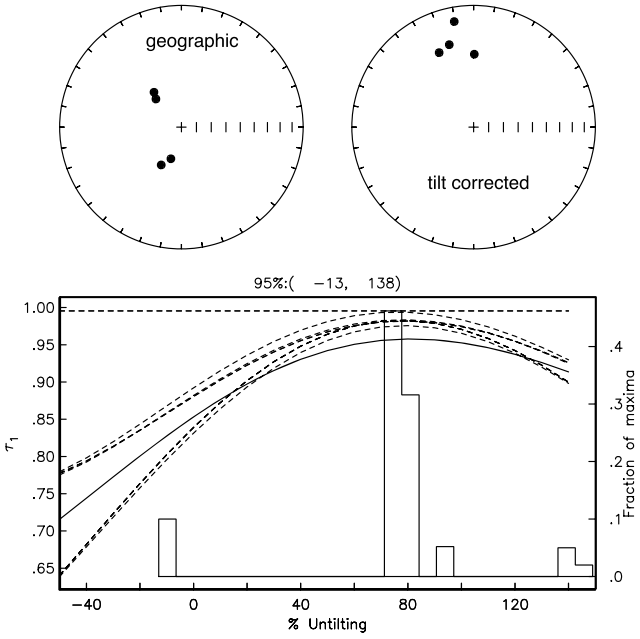

Figure 8. Nonparametric fold test [*Tauxe and Watson*, 1994] for the extrusive sequence of the Sarıkaraman ophiolite. Stereonets show the site mean ChRM directions before (geographic) and after tilt correction for the four pillow lava sites. Below is the result of the fold test with bootstrapped statistics on the first eigenvalues ($\tau 1$) upon progressive untilting. The 95% bootstrap error interval is indicated. Best grouping is reached between 80 and 100% unfolding.

to be pre-tilt (and likely primary). This has been confirmed at least for the pillow basalts by the positive result of a nonparametric fold test [*Tauxe and Watson*, 1994], indicating maximum clustering between 80 and 100% unfolding (Figure 8).

We exclude that the seafloor metamorphism affecting these rocks could have overprinted the original remanence, due to the low temperature of this process (<300°C) compared to the high Curie temperatures of the sampled rocks (>350°C). More importantly, magnetizations acquired during seafloor metamorphism can be considered as primary because this process operates soon after rocks have acquired a (primary) thermoremanent magnetization at the spreading ridge.

A mean tilt-corrected direction with declination (D) = 348.4° ± 4.5° and inclination (I) = 33.2° ± 6.7° (K = 20.6; A_{95} = 4.3°) was calculated for the extrusive sequence by combining sites SAR07, SAR08, SAR09, and SAR10 (Table 3 and Figure 7). This indicates a minor (~12°) counterclockwise vertical axis rotation of the ophiolite since circa 90 Ma, which is comparable to the rotation of the African plate in the same time span [*Torsvik et al.*, 2012].

The tilt-corrected direction from the pillow basalts was used to select the reference direction for the net tectonic rotation analysis (D = 000°, and I = 33.2°, α_{95} = 4.6°). Net tectonic rotation analysis was performed using single site mean paleomagnetic directions from the sheeted dike sites. Given the consistency of their directions, a mean paleomagnetic direction for sites SAR01, SAR02, and SAR03 was used instead of their single directions (Table 3). Two permissible solutions were obtained at all sites except SAR06, where the dikes could not be restored to the vertical (Table 4). Site SAR06 was therefore discarded from further analyses.

Preferred solutions were selected based on the regional tectonics (minor counterclockwise rotations and overall northward tilt) inferred from the pillow basalts, as well as the distribution of the different ophiolite units within the sampling area (gabbros to the south, sheeted dikes in the center, and lavas to the north). The preferred net tectonic rotation solutions (Table 4) indicate counterclockwise rotations by 35–65° around

Table 4. Solutions of the Net Tectonic Rotation Analysis are Expressed as Azimuth and Plunge of the Rotation Axis, Amount and Sense of Rotation, and Strike and Dip of the Restored Dikes[a]

		Preferred Solution						Alternative Solution					
Site	Lithology	Azimuth (deg)	Plunge (deg)	Rotation (deg)	Sense	Initial Strike (deg)	Initial Dip (deg)	Azimuth (deg)	Plunge (deg)	Rotation (deg)	Sense	Initial Strike (deg)	Initial Dip (deg)
SAR01-02-03	Sheeted dikes	017.0	42.8	65.8	CCW	020	90	353.8	41.3	139.2	CW	160	90
SAR04	Sheeted dikes	075.1	36.7	68.2	CCW	012	90	340.5	59.9	159.0	CW	167	90
SAR05	Sheeted dikes	198.5	53.9	35.1	CW	352	90	021.2	36.0	170.9	CCW	008	90
SAR06*	Sheeted dikes	140.3	20.0	93.5	CCW	090	70	-	-	-	-	-	-

[a]Rotation sense as clockwise (CW) or counterclockwise (CCW) is indicated. The initial dike strike and dip obtained from the analysis at each site (or group of sites) is shown.

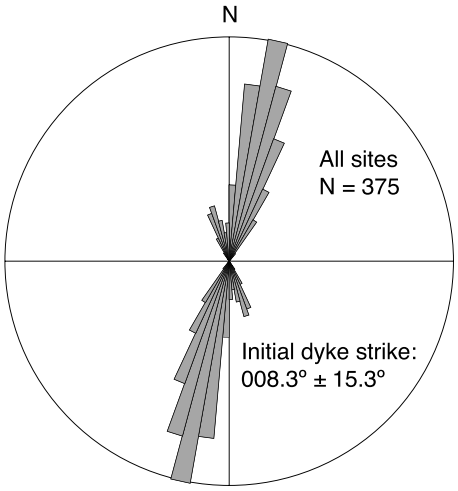

Figure 9. Rose diagram distribution of the permissible initial dike strike of the Sarıkaraman ophiolite obtained from the net tectonic rotation analysis once the errors on the paleomagnetic vectors, dike orientation, and reference direction are considered.

moderately plunging (40–55°) axes. The initial dike orientations from the preferred solutions are strongly consistent, and when the errors are modeled following method described by *Morris et al*. [1998], they show a predominant ~ N-S (azimuth = 008 ± 15°) direction (Table 4 and Figure 9). The results from the net tectonic rotation analysis therefore indicate a ~ N-S trending paleo-ridge with a ~ E-W spreading direction.

5. Discussion

5.1. Timing of Subduction Initiation and Accretion of the Central Anatolian Metamorphic Belts

Our compilation of geochronological data was used to constrain the timing of plutonism and metamorphism in the crystalline massifs of Central Anatolia contains (i) U/Pb ages from zircon in granitoids, Re/Os molybdenite ages, and Lu/Hf garnet ages, which were all interpreted as mineral growth ages by the original authors; (ii) Titanite U/Pb ages are assumed to represent cooling below ~660–700°C [*Scott and St-Onge*, 1995]; (iii) $^{40}Ar/^{39}Ar$ ages are interpreted as cooling ages, with assumed closure temperatures of ~500°C for hornblende [*Harrison*, 1981], ~400°C for muscovite and phengite [*Harrison et al*., 2009], ~300–350°C for biotite [*Grove and Harrison*, 1996], and ~200–250°C [*Harrison and McDougall*, 1982; *McDougall and Harrison*, 1999] or ~300–375°C for K feldspar [*Cassata and Renne*, 2013] (Table 1).

The overview of age constraints in Figures 2 and 3, and Table 1, shows a consistent pattern. First, metamorphic soles below widespread klippen of ophiolites give hornblende and locally muscovite $^{40}Ar/^{39}Ar$ cooling ages of circa 93 ± 3 Ma across most of Turkey. Subophiolitic metamorphic soles are widely interpreted to start forming shortly after subduction initiation, at temperatures up to 800°C and pressures up to 10–15 kbar [*Önen and Hall*, 1993; *Dilek and Whitney*, 1997; *Hacker and Gnos*, 1997; *Plunder et al*., 2015]. The ages recorded by $^{40}Ar/^{39}Ar$ thermochronology on hornblende represent cooling below ~500°C, i.e., at greenschist facies conditions, during decompression and exhumation of the metamorphic soles, likely related to SSZ spreading and subsequent tectonic thinning and attenuation of the mantle wedge [*van Hinsbergen et al*., 2015]. Formation of SSZ oceanic crust occurs at the expense of a still hot mantle close to the trench and therefore appears limited to the first 5–10 Myr of an intraoceanic subduction zone [e.g., *Stern et al*., 2012]; similar time periods after subduction initiation were estimated for the formation of metamorphic soles [*Hacker*, 1990]. From this, it follows that subduction initiation below the Anatolian ophiolites probably occurred at circa 100 Ma.

A few outlier ages are clear from Figure 3. Ophiolites north of the Kırşehir Block yield Jurassic metamorphic sole and gabbro ages and may relate to an earlier obducted ophiolite that connected to the contemporaneous Hellenic-Dinaric ophiolites [*Çelik et al*., 2013; *Topuz et al*., 2013]. *Parlak et al*. [2013] reported a circa 69 Ma U/Pb zircon age from a gabbro in the Karsantı ophiolite and interpreted this to reflect the age of ocean floor formation. In several places, however, post kinematic mafic dikes intrude the metamorphic soles and the Anatolian ophiolites [*Cakir et al*., 1978; *Lytwyn and Casey*, 1993; *Parlak and Delaloyle*, 1996; *Parlak*, 2000; *Çelik and Delaloyle*, 2003; *Parlak et al*., 2006; *Çelik*, 2008], with ages ranging from circa 90 to 65 Ma [*Parlak and Delaloyle*, 1996; *Çelik*, 2007, 2008]. We suspect that the young U/Pb age represents post kinematic gabbroic intrusions fed by the Upper Cretaceous dikes that cut the metamorphic soles and do not reflect the spreading stage of the oceanic crust of the ophiolites.

The circa 85 Ma U/Pb ages on monazite in the migmatites from the Kırşehir Massif are interpreted as ages of peak regional metamorphism [*Whitney et al*., 2003; *Whitney and Hamilton*, 2004]. In addition, a migmatitic gneiss in Nigde massif yielded a circa 91 Ma U/Pb age [*Whitney and Hamilton*, 2004], suggesting that by that time the Kırşehir Block was already undergoing metamorphism. Regional pervasive shearing ceased at the peak of regional metamorphism. Subsequently, granitoids with U/Pb ages of 85–73 Ma cut the regional

foliation, accompanied between 78 and 73 Ma by molybdenite mineralizations [*Delibaş and Genç*, 2012b]. $^{40}Ar/^{39}Ar$ cooling ages of granitoids and schists regionally range between circa 80 and 65 Ma (Figure 2 and Table 1) and thus show significant overlap with the ages of granitoid intrusion, consistent with a syn-exhumational character of the granitoids inferred from geochemical arguments [*İlbeyli*, 2005; *Köksal et al*., 2013] and structural crosscutting relationships [*Lefebvre et al*., 2011]. Nonmetamorphosed "Karahıdır volcanics" in the Ayhan basin [*Advokaat et al*., 2014] and in the northwest of the Kırşehir massif (point 76, Figure 2) give ages of circa 72 Ma and were likely deposited in supradetachment basins during extensional exhumation.

The ophiolites overlying the Kırşehir Block give ages overlapping with or older than peak regional metamorphic ages. They also give ages older than the granitoid intrusion and regional cooling ages: plagiogranite U/Pb crystallization ages in plagiogranite from the Sarıkaraman ophiolite are 89–90 Ma. Plagioclase yielded a 85 Ma $^{40}Ar/^{39}Ar$ age for the Kurancalı gabbro (Figure 2 and Table 1). The nonmetamorphic character of the Sarıkaraman ophiolite (dikes, pillow lavas, and sediments) and 10–15 Ma older cooling age of the Kurancalı gabbro compared to the cooling ages of the underlying Kırşehir metamorphics demonstrate that these crustal ophiolitic rocks did not share the burial and metamorphic history of the Kırşehir Block. Instead, they remained at much shallower crustal levels. Their present-day contact with the Kırşehir metamorphics must represent an extensional detachment, intruded by granitoids, as well documented for the Kaman detachment west of Kurancalı [*Lefebvre et al*., 2011]. The 89–90 Ma ages of the plagiogranites of the Sarıkaraman ophiolite (Figure 5), moreover, show that the ophiolite still underwent magmatic spreading when most of the metamorphic soles to the west and south in ophiolites overlying the Taurides were already exhumed to depths corresponding to greenschist facies conditions.

As little as 4–5 Myr after the magmatic spreading of the Sarıkaraman ophiolitic crust ceased, the Kırşehir Block reached peak pressure conditions and stopped being regionally sheared. We interpret this moment as its final decoupling from the downgoing plate and its accretion to the overriding oceanic lithosphere of which the Sarıkaraman ophiolite is a relict. Subsequently, both the host to a magmatic arc that remained stable for circa 15 Myr (Figure 2), showing that mantle influx became possible when the Kırşehir Block crust decoupled from its original underlying lithospheric mantle, which continued to subduct and formed the slab. Modern typical arc-trench distances are on the order of 150–200 km [e.g., *Gill*, 1981]; the Sarıkaraman ophiolite thus likely formed in a location close to that distance away from the trench. The age difference between the crystallization of this ophiolite and the cooling ages of the metamorphic soles likely reflects the hinterland migration of the spreading center away from the subduction zone above which the Anatolian SSZ ophiolites were forming [*van Hinsbergen et al*., 2015]. This relationship also suggests that the subduction angle at which the Kırşehir Block underthrusted the Sarikaraman Plate was very low: the Kırşehir Block reached a depth of only ~25 km but was already in an arc position, hence some 150 km away from the trench, immediately after its decoupling from the downgoing plate and at the inception of extensional exhumation.

Phengite $^{40}Ar/^{39}Ar$ and Rb/Sr ages of the Tavşanlı zone of 88–78 Ma, likely just postdate peak pressure metamorphism, and the end of burial and accretion of the Tavşanlı zone to the overriding plate (Figure 3 and Table 1). A recent Lu/Hf garnet ages from a lawsonite eclogite of the Tavşanlı zone yielded a circa 91 Ma age [*Mulcahy et al*., 2014]. This age is synchronous with the oldest U/Pb age of zircon in high-grade migmatites of the Kırşehir Block [*Whitney and Hamilton*, 2004]. Younger ages close to 60 Ma may result from reheating by Barovian metamorphism [*Seaton et al*., 2009, 2014]. The age of HP-LT metamorphism of the Tavşanlı zone therefore overlaps with the ages of peak regional metamorphism and magmatism in the Kırşehir Block. The two complexes were buried and metamorphosed simultaneously below ophiolites of similar age. With metamorphic sole ages around 95 Ma and subduction having started a few million years before that continental subduction burying the Kırşehir Block and Tavşanlı zone must have occurred within 10 Ma after intraoceanic subduction initation [*Kaymakci et al*., 2009].

Finally, the Afyon zone yielded phengite $^{40}Ar/^{39}Ar$ ages of 60–65 Ma [*Özdamar et al*., 2013; *Pourteau et al*., 2013], interpreted to reflect postpeak metamorphism cooling during the early stages of exhumation following the accretion of the Afyon zone from the downgoing to the overriding plate. The underthrusting of the Afyon zone and its subsequent accretion to the overriding orogen thus occurred simultaneously with the exhumation of the Kırşehir Block along E-W extensional detachments [*Gautier et al*., 2008; *Lefebvre et al*., 2011, 2015].

The youngest sediments incorporated in the structurally deepest units of the Taurides (Figure 1) are Eocene platform carbonates and overlying flysch [*Monod*, 1977; *Özgül*, 1984]. It shows that the continental subduction continued until at least this time, after which oceanic lithosphere of the eastern Mediterranean basin, south of the Taurides, became subducted. The thin-skinned nature of deformation throughout Anatolia shows that the lower crustal and mantle underpinnings of the original Anatolide-Tauride continent must have subducted and that the arrival of continental lithosphere in the southern Anatolian trench in the Cretaceous did not lead to arrest of subduction and slab breakoff.

5.2. Burial and Exhumation History of the Kırşehir Block

During the 15 Myr between subduction initiation and the onset of post kinematic granitoid intrusion in the Kırşehir Block the regional foliation and lineation of the Kırşehir metamorphics were formed. We postulate that the regional foliation and sense of shear developed during the northeastward underthrusting of the Kırşehir Block, as part of the African Plate, below the oceanic lithosphere of the Anatolian ophiolites. In other words, we interpret the regional peak metamorphic conditions of the Kırşehir Block as prograde metamorphism reaching 7–8 kbar and 700°C, which for a subduction zone is anomalously hot. These hot conditions weakened the Kırşehir metamorphic rocks and distributed the underthrusting-related shear throughout the block leading to the regional shear foliation and the consistent top-to-the-SW sense of shear (corrected for Cenozoic vertical axis rotations).

The ophiolites that overlie the Kırşehir Block currently only form isolated fragments, no more than some 100 s of meters thick, and with a highly dismembered ophiolitic pseudostratigraphy. These ophiolites must have formed part of a 20–25 km thick oceanic plate and underlying mantle wedge when the Kırşehir metamorphic rocks recorded their peak pressure conditions (7–8 kbar). This oceanic lithosphere and mantle wedge must thus have been dramatically stretched and thinned, to the extent that the rocks underlying the wedge, i.e., the Kırşehir Block, became exhumed to the surface. In that context it is interesting to note that the E-W extension direction during spreading of the oceanic crust of the Sarıkaraman ophiolite as inferred from our paleomagnetic work (Figure 9) is similar to the extension direction associated with the extensional detachments between Kırşehir metamorphic rocks and the Central Anatolian Ophiolites [*Gautier et al*., 2008; *Lefebvre et al*., 2011, 2015; *Advokaat et al*., 2014].

Gautier et al. [2008] and *Lefebvre* [2011] previously interpreted the regional foliation and top-to-the-SW shearing to have formed coevally with top-to-the-E and top-to-the-W detachments and considered the former the result of lower crustal flow into exhuming domes. Although we instead invoke that the top-to-the-SW sense of shear reflects the burial of the Kırşehir metamorphics, we note that E-W overriding plate extension and top-to-the-SW sense of shear associated with burial were indeed coeval, at least around 90 Ma. The Kırşehir Block was essentially subducted below an active spreading ridge that was spreading at high angles relative to the subduction direction. At around 90 Ma, E-W overriding plate extension still caused magmatic spreading, but soon thereafter it was likely accommodated by nonmagmatic "ophiolite hyperextension" [*Maffione et al*., 2015b], fragmenting and dismembering the Anatolian ophiolites to such an extent that subophiolitic mélange, and even underlying Kırşehir metamorphic rocks were exhumed to the surface. This may explain in part why the Kırşehir Block was never buried deeply: spreading in the overriding lithosphere thinned the mantle wedge during underthrusting led to formation of a flat slab. A similar mechanism was recently proposed to explain syn-formational exhumation of metamorphic soles [*van Hinsbergen et al*., 2015].

For the Kırşehir Block, formation of the regional foliation was completed prior to the 85 Ma onset of granitoid intrusion, at which time the crust of the Kırşehir Block must have been decoupled from its mantle lithosphere, and transferred as a nappe from the downgoing African plate to the base of the overriding oceanic plate as already proposed for the Aegean region [*van Hinsbergen et al*., 2005]. The Kırşehir Block was intruded by arc magmas soon after its mantle lithosphere delaminated from the crust, and the slab must thus have steepened rapidly, allowing inflow and decompression of already hydrated mantle below the Kırşehir Block. This caused the melting and intrusion of the granitoid belts, consistent with previous inferences from geochemistry [*İlbeyli*, 2004a, 2004b, 2005; *Kadıoğlu et al*., 2006; *İlbeyli et al*., 2009; *Köksal et al*., 2012]. Slab steepening further enhanced E-W overriding plate extension which in the Kırşehir Block continued until after 66 Ma and before the mid-Eocene [*Advokaat et al*., 2014]. The locus of extension then migrated westward toward the Tuzgölü Basin [*Cemen et al*., 1999; *Aydemir and Ates*, 2006, 2008; *Fernandez-Blanco et al*., 2013] and the Konya area [*Koç et al*., 2012, 2016b].

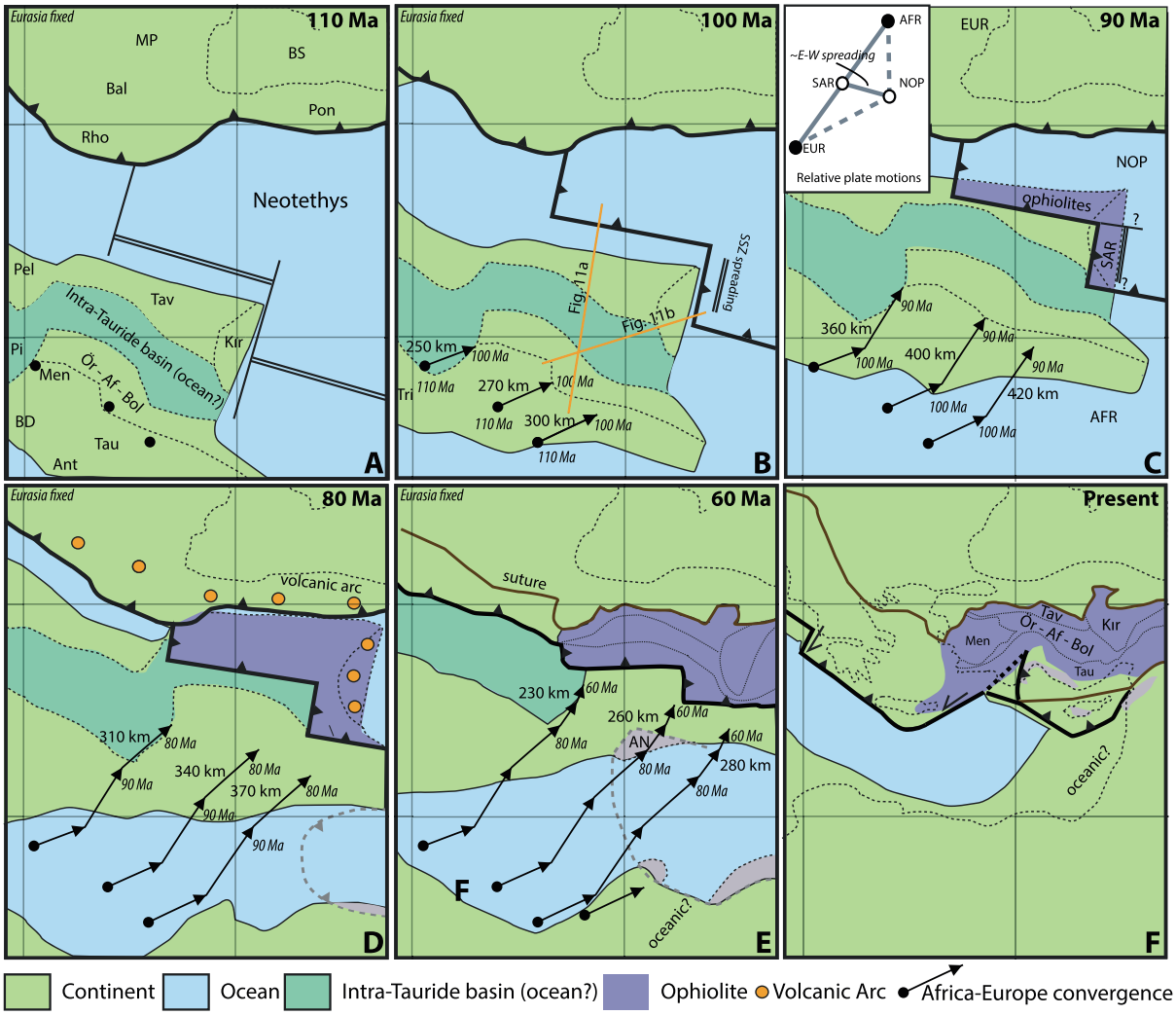

Figure 10. Paleogeography and plate boundary configuration of Central Anatolia between from 110 to 60 Ma. Paleogeography of the Aegean and west Anatolian region after *van Hinsbergen and Schmid* [2012], *Gaina et al.* [2013], and *Vissers et al.* [2013]; Antalya nappe emplacement history after *Moix et al.* [2008] and *Cetinkaplan et al.* [2016]; see text for further explanation. AFR = Africa; AN = Antalya nappes; Bal = Balkanides; BD = Bey Dağları; BS = Black Sea; EUR = Europa; ITB = conceptual Intra-Tauride basin; Kır = Kırşehir Massif; Men = Menderes massif; MP = Moesian platform; NOP = Neotethyan Oceanic Plate(s); Ör-Af-Bol = Ören-Afyon-Bolkardağ zone; Pel = Pelagonian platform; Pi = Pindos basin; Pon = Pontides; Rho = Rhodope; SAR = Sarıkaraman microplate; Tau = Tauride carbonate platform; Tav = Tavşanlı zone; and Tri = Tripolitza; inset in Figure 10c: possible plate motion vectors in velocity space [see *Cox and Hart*, 1986], illustrating the relative motions between the minimum of four (micro-)plates that governed the kinematic history of Central Anatolia around 90 Ma; see text for further explanation.

5.3. Cretaceous Plate Kinematics and Central Anatolian Tectonics

Using the Eurasia-North America-Africa plate circuit of *Torsvik et al.* [2012], the total amount of plate convergence between 100 and 60 Ma for a location in south-central Turkey (modern coordinate 30°N/35°E) is ~1000 km, with Africa moving to the NE relative to Eurasia. The bulk of this convergence is accommodated between 100 and 80 Ma (~750 km, i.e., 3.8 cm/yr) and decreased to ~1.3 cm/yr after 80 Ma. Between 80 Ma and the present, ~1100 km of convergence have occurred, 250 km of which took place during the time span in which the Afyon zone was buried, sometime between 80 and 60 Ma (Figure 10).

At least two other plates must have existed between the African and Eurasian plates, when the Sarıkaraman ophiolite was forming at a spreading center, i.e., around 90 Ma (Figure 10). These two conceptual plates, depicted as "Sarıkaraman microplate (SAR)" and the "Neotethyan Oceanic Plate (system) (NOP)" that must have underlain the remainder of the Neotethyan oceanic realm (Figure 10) were separated by a N-S striking ridge paleomagnetically reconstructed from the Sarıkaraman sheeted dikes (Figure 9). The Sarıkaraman microplate was separated from the African plate by a trench at which the African plate subducted

northnortheastward, and the Neotethyan Oceanic Plate subducted below Eurasia south of the Pontides. We illustrate the relative motions of these plates in a conceptual plate motion diagram in velocity space (Figure 10f). NOP moves eastward relative to SAR as determined by the N-S orientation of the Sarıkaraman sheeted dikes. The shear sense indicators that formed on the foliation during burial and regional metamorphism of the Kırşehir Block, when corrected for Cenozoic vertical axis rotations, are consistently top-to-the-SW [*Lefebvre*, 2011; *Lefebvre et al*., 2013]. We interpret this to indicate the relative motion between Africa (AFR) and SAR, from which it follows that the convergence angle between AFR and NOP was more or less N-S, and the convergence angle between NOP and Europe (EUR) was NE-SW, with the exact angle depending on the spreading rate between SAR and NOP.

The sharp kink in the strike of the Cretaceous intraoceanic subduction zone, between ~ N-S and ~ E-W segments proposed earlier [*Advokaat et al*., 2014] was interpreted to result from subduction initiation along an ~ E-W ridge and ~ N-S transform system [*van Hinsbergen et al*., 2015] (Figure 10). This subduction zone geometry would result in a highly oblique N-S trending subduction zone in Central Anatolia along which the Kırşehir Block was underthrust, whereas the Tavşanlı zone subducted nearly orthogonally along an E-W trending trench. If our inferences of the spreading direction between SAR and NOP are correct, subduction below the Pontides was, at least around 90 Ma, also sinistral oblique.

5.4. Central Anatolian Paleogeography

Some authors view the Kırşehir Block as the contiguous northern promontory of the Tauride platform [e.g., *Boztuğ et al*., 2009c; *Köksal et al*., 2013], but most suggested that the Kırşehir Block was separated from the Tauride block by an oceanic basin, conceptually termed the "Intra-Tauride Ocean" [*Sengör and Yilmaz*, 1981; *Görür et al*., 1984; *Okay*, 1984; *Okay et al*., 1996]. Moreover, the ophiolites that overlie the Taurides as well as the Afyon zone (Figure 3) are widely interpreted to have formed following intraoceanic subduction within this intra-Tauride Ocean, whereas the Central Anatolian Ophiolites overlying the Kırşehir Block are interpreted to result from a time equivalent but separate subduction zone within the Neotethys Ocean [*Dilek et al*., 1999; *Andrew and Robertson*, 2002; *Barrier and Vrielynck*, 2008; *Robertson et al*., 2009; *Pourteau et al*., 2010; *Parlak et al*., 2013].

We perceive no argument for a double Cretaceous subduction system in Central Anatolia. First, the age of burial and metamorphism along a transect from the Tavşanlı zone to the south or from the Kırşehir Block to the west becomes progressively younger. This can be straightforwardly explained by progressive in-sequence, foreland-propagating nappe stacking in a single subduction zone (Figure 11), similar to well-documented Aegean and west Anatolian examples [*van Hinsbergen et al*., 2005, 2010], or to the Alps [*Handy et al*., 2010]. Second, shortly after the accretion of the Kırşehir Block to the Sarıkaraman microplate, both became intruded by volcanic arc magmas. Typical arc-trench distances suggest that the underthrust Kırşehir Block and overlying ophiolites were separated by a 150–200 km wide fore-arc floored by the Sarıkaraman microplate. Relics of this fore-arc are the Haymana, Tuzgölü, and Ulukışla basins fringing the Kırşehir Block to the west and south [*Görür et al*., 1984; *Kocyigit*, 1991; *Clark and Robertson*, 2002]. The present distance between the Kırşehir Block and the ophiolites in the Tauride mountains, e.g., the Beyşehir Ophiolite (BO; Figure 3), is ~250 km, which represents this original fore-arc width plus the amount of extension that has been accommodated in the Tuzgölü basin. This amount of extension remains unquantified, but given the widespread exposure of exhumed HP-LT metamorphic Afyon zone rock, it may be considerable. As illustrated in Figures 10 and 11, a single but kinked subduction zone below oceanic lithosphere formed an ophiolite sheet as a roof thrust over a foreland-propagating series of nappes from the Tavşanlı zone and Kırşehir Block in the north and east, via the Afyon zone, to the Taurides in the south and west. This subduction zone retreated relative to the overriding plate to the south and west and exhumed previously underthrusted units in the back arc, comparable to, e.g., the Alboran domain, the Calabrian-Tyrrhenian system, or the Aegean-west Anatolian region [*Jolivet et al*., 2003; *Rosenbaum and Lister*, 2004; *Jolivet et al*., 2009; *van Hinsbergen and Schmid*, 2012; *Faccenna et al*., 2014; *van Hinsbergen et al*., 2014]. Contraction and extension migrated toward the foreland, which has reached as far as the Bey Dağları platform [*Koç et al*., 2016a, 2016b] (Figure 1). There is no evidence that ophiolites underthrust the Tavşanlı zone or Kırşehir Block, nor are there parallel metamorphic zones of the same age or parallel arcs that would require a more complex subduction zone configuration than the one outlined in Figure 10.

This, of course, does not exclude that an Intra-Tauride ocean basin once existed. If it did, it must have subducted in the period between the accretion of the Kırşehir Block around 85 Ma and the Afyon zone around

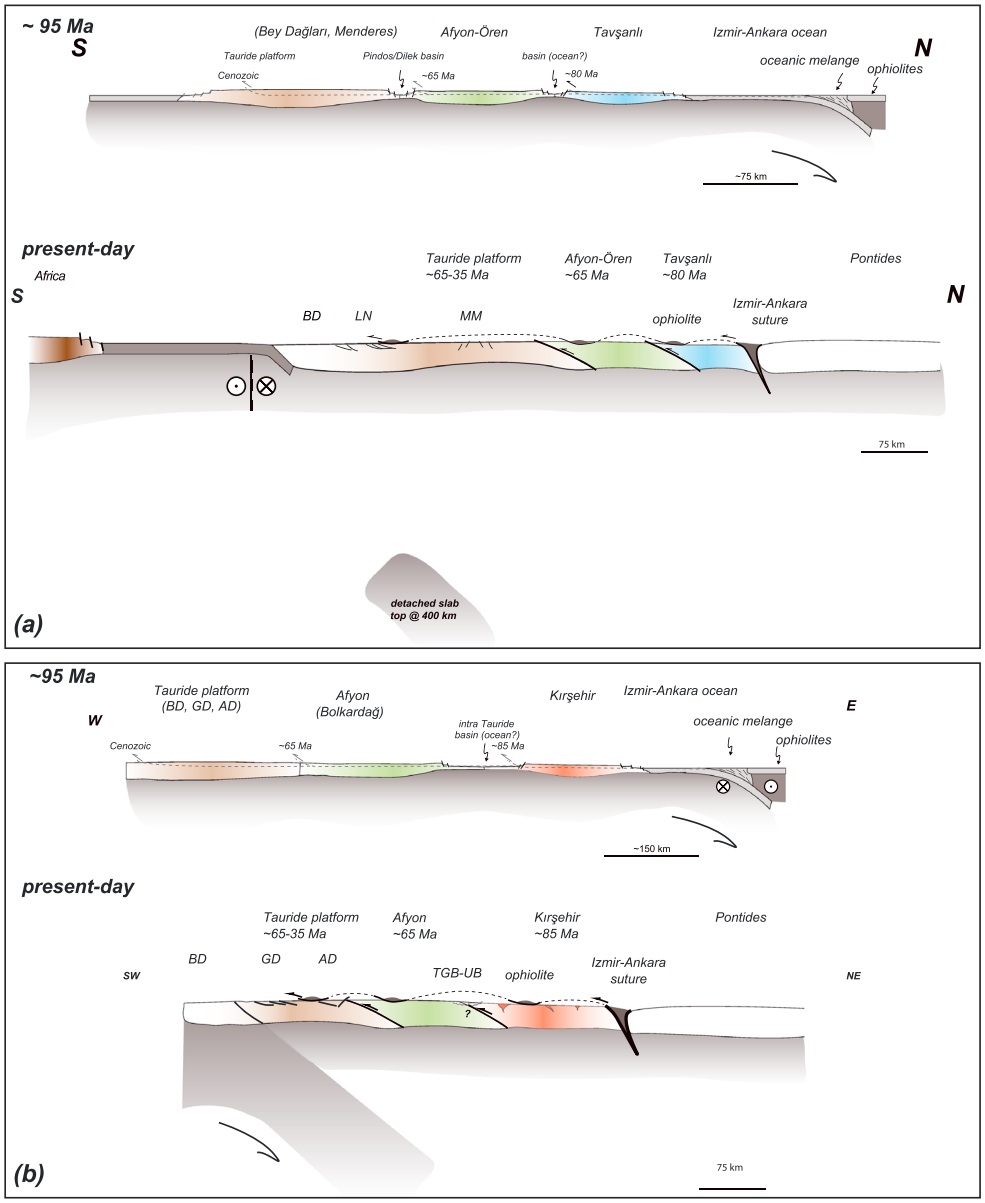

Figure 11. Lithospheric cross sections shortly after subduction initiation and present-day. (a) N-S cross section from the Tavşanlı zone to the Taurides. (b) E-W cross section from the Kırşehir Block to the Taurides (present-day section oriented NE-SW). See Figure 10a for approximate location. Dotted thrusts illustrate the foreland propagation of accretion of the various zones through time to the overriding oceanic lithosphere of the south Anatolian subduction system. (Abbreviations used: AD, Aladağ; BD, Bey Dağları; GD, Geyikdağ; LN, Lycian nappes; MM, Menderes massif, TGB, Tüz-Gölü basin; and UB, Ulukışla basin). For the interpretation of the present-day section, see *van Hinsbergen et al*. [2010] and *Biryol et al*. [2011].

65 Ma (Figure 11), i.e., in the time interval of the formation of the granitoid belt that intruded the Kırşehir Block and during its extensional exhumation. Our plate kinematic reconstruction demonstrates that in this time period, a total of 450 km of Africa-Europe convergence was accommodated, and this was partitioned over two subduction zones. The E-W subduction component of this convergence was ~200 km. The amount of Cretaceous E-W extension that exhumed the Kırşehir Block, which is equal to its exhumed width of 100 km may be added to this. This would give a maximum width of an Intra-Tauride ocean of ~300 km west of the Kırşehir Block and a similar dimension south of the Kırşehir Block and between the Tavşanlı and Afyon zones. We are, however, not aware of any demonstrable geological record of such an ocean basin. The geochemistry

of the granitoids may hold evidence for oceanic subduction below the Kırşehir Block. In addition, an Intra-Tauride ocean would have to be invoked if oceanic sediments of 85–65 Ma would be found in the subophiolitic mélange of the central Taurides.

5.5. Subduction Obliquity Determined Thermal Evolution of Plate Contact?

A final point of discussion is the major difference in prograde and peak metamorphic grade between the Kırşehir Block and the Tavşanlı zone. The magmatic arc that intruded the Kırşehir Block is not likely to have caused the regional HT metamorphism: all arc-related plutons are essentially undeformed and intrude the syn-HT regional foliation that appears to have only affected metasedimentary rocks. The intrusion of the arc did cause a syn-decompressional thermal pulse at 3–4 kbar/650–800°C post dating peak pressure metamorphic conditions at 8 kbar [*Whitney and Dilek*, 1998, 2001; *Lefebvre*, 2011; *Lefebvre et al*., 2015]. We therefore interpret the regional deformation to be caused by burial, and from that conclude that burial occurred at much higher temperatures than normal for subduction systems, while at the same time to the west, the Tavşanlı zone experienced burial associated with regular HP/LT metamorphism.

The Kırşehir Block and the Tavşanlı zone units likely being lateral equivalents of the same continental block and in any case underthrust simultaneously below oceanic lithosphere of similar age. Why did the Kırşehir Block experience high temperatures at medium pressures and the Tavşanlı zone low temperatures at high pressures? In addition, why is the younger Afyon zone more homogeneous in its metamorphic grade? How can such high temperatures have been reached in the Kırşehir Block so soon after its burial, with so little convergence and hence potential shortening and crustal thickening?

We suggest that the obliquity of subduction may have played a key role. The Kırşehir Block underthrust highly obliquely below a N-S trending subduction zone, whereas the Tavşanlı zone underthrust near orthogonally (Figure 10). The rate of burial of the Tavşanlı zone was therefore much higher than of the Kırşehir Block, which consequently had more time to heat up due to underthrusting below a mantle that was hot enough to partially melt and generate oceanic crust. In addition, the overriding plate extension by spreading of the Sarıkaraman ophiolite may have actively prevented the Kırşehir Block from underthrusting steeply. This is strengthened by the back-arc spreading induced in high oblique convergence system as previously documented in the Sunda region [*Kimura*, 1986].

By the time the Afyon zone was underthrusting, several key factors may have changed. First, the plate convergence rate had dropped to ~1 cm/yr, which would have decreased the contrast in thermal history between the N-S and E-W trending systems. In addition, the westward rollback of the N-S trending subduction zone, which caused E-W extension in the Kırşehir Block and the area to the west, may have accelerated over time, which would have decreased the subduction obliquity. Finally, the temperature highest in a juvenile subduction zone decreases over time [e.g., *Lázaro et al*., 2009; *Plunder et al*., 2013]. To further unravel the causes of different thermal regimes in Anatolia, it is essential to accurately reconstruct the amount, timing, and direction of extension associated with exhumation of metamorphic rocks in Central Anatolia, in particular of the Afyon and Tavşanlı zones.

6. Conclusions

In this paper, we review structural, metamorphic, and geochronological constraints on the tectonic history of Central Anatolia and place them in a plate kinematic context of Africa-Europe convergence since the Cretaceous to restore a first-order paleogeography of oceans and continents. To this review, we add new $^{40}Ar/^{39}Ar$ and U/Pb ages from the Kırşehir Block and the overlying Sarıkaraman suprasubduction zone ophiolite. We also show paleomagnetic evidence from the sheeted dike section of the Sarıkaraman ophiolite to restore the orientation of the spreading ridge during the formation of the oceanic crust. Our conclusions are summarized as follows:

1. The geology of Central Anatolia can be successfully explained by the synchronous activity of two subduction zones, one below the Pontides and one intraoceanic subduction zone within the Neotethys. The latter likely started to form around 100 Myr and was associated with overriding plate spreading and synchronous metamorphic sole exhumation until circa 90 Ma. The youngest oceanic crust is found in the Sarıkaraman ophiolite in an arc position, with new ages of circa 90 Ma. The intraoceanic subduction zone had E-W and N-S striking segments, likely inherited from an inverted ridge-transform configuration.

2. Continental subduction of the Anatolide-Tauride platform occurred below the oceanic lithosphere of the southern subduction system. This led to accretion of crust from the downgoing plate to the overriding plate in a foreland-propagating nappe stack with the oldest nappe system far underthrusted and metamorphosed below the oceanic lithosphere of the overriding plate. This lithosphere is preserved as extensionally and erosionally dismembered ophiolites. The oldest nappes to accrete were the Kırşehir Block and Tavşanlı zone both accreting around 85 Ma, followed by the Afyon zone, which was accreted around 65 Ma, and the nappes of the nonmetamorphosed Taurides, which were accreted until at least Eocene time. There is no argument to invoke yet another subduction system within the conceptual "Intra Tauride ocean" between the Kırşehir Block/Tavşanlı zone and the Afyon zone.
3. If an Intra Tauride Ocean existed, plate kinematic constraints limit its width to 300 km. It would have subducted between 85 Ma and 65 Ma. No geological record has been identified to date that demonstrates the existence of such an ocean basin, but indications may be found in subduction-related plutons in the Kırşehir Block that formed between 85 and 70 Ma.
4. Central Anatolia exhibits a long history of E-W overriding plate extension. Our paleomagnetic evidence shows that the spreading center forming the Sarıkaraman ophiolite at 90 Ma was E-W spreading. The Kırşehir Block was exhumed by E-W extension, the Tuzgölü Basin formed by E-W extension in the Paleogene onward, and E-W extension has been active since the Miocene in the Central Taurides, where it remains active today. We ascribe this to the westward retreat of the ~N-S striking Kırşehir subduction segment since the Cretaceous.
5. High-temperature, low-pressure metamorphism in the Kırşehir Block and high-pressure, low-temperature metamorphism in the Tavşanlı zone were synchronous. We tentatively explain this difference by their angle of subduction. The Tavşanlı zone subducted at a high angle and was buried at plate convergence rates leading to deep burial at low temperatures. The Kırşehir Block subducted highly obliquely at low burial rates, allowing a higher increase in temperature. Its underthrusting below the actively spreading Sarıkaraman ridge likely prevented deep burial and led to decompression and exhumation during underthrusting.

Appendix A

Procedures and analytical details of previously unpublished $^{40}Ar/^{39}Ar$ and U/Pb ages included in the compilation of Table 1 and Figures 2 and 3.

Acknowledgments

D.J.J.v.H., M.M., A.P., D.G., and E.L.A. acknowledge financial support through ERC Starting grant 306810 (SINK) to D.J.J.v.H. D.J.J.v.H., K.P., and P.J.McP. acknowledge funding through NWO VIDI grant 864.11.004 to D.J.J.v.H. The data used are listed in the references, tables, and supplements. We thank Laurent Jolivet, Aral Okay, and an anonymous reviewer for their useful comments.

References

Advokaat, E. L., D. van Hinsbergen, N. Kaymakci, R. L. M. Vissers, and B. W. H. Hendriks (2014), Late Cretaceous extension and Palaeogene rotation-related contraction in Central Anatolia recorded in the Ayhan-Büyükkışla basin, *Int. Geol. Rev.*, *56*, 1813–1836.

Aldanmaz, E., M. W. Schmidt, A. Gourgaud, and T. Meisel (2009), Mid-ocean ridge and supra-subduction geochemical signatures in spinel–peridotites from the Neotethyan ophiolites in SW Turkey: Implications for upper mantle melting processes, *Lithos*, *113*, 691–708.

Allerton, S., and F. J. Vine (1987), Spreading structure of the Troodos ophiolite, Cyprus: Some paleomagnetic constraints, *Geology*, *15*(7), 593–597.

Altiner, D., İ. Ömer Yilmaz, N. Özgül, N. Akçar, M. Bayazitoğlu, and Z. E. Gaziulusoy (1999), High-resolution sequence stratigraphic correlation in the Upper Jurassic (Kimmeridgian)–Upper Cretaceous (Cenomanian) peritidal carbonate deposits (Western Taurides, Turkey), *Geol. J.*, *34*, 139–158.

Andrew, T., and A. H. Robertson (2002), The Beyşehir–Hoyran–Hadim Nappes: Genesis and emplacement of Mesozoic marginal and oceanic units of the northern Neotethys in southern Turkey, *J. Geol. Soc.*, *159*, 529–543.

Anonymous (1972), Penrose field conference on ophiolites, *Geotimes*, *17*, 24–25.

Aydemir, A., and A. Ates (2006), Structural interpretation of the Tuzgolu and Haymana Basins, Central Anatolia, Turkey, using seismic, gravity and aeromagnetic data, *Earth Planets Space*, *58*, 951–961.

Aydemir, A., and A. Ates (2008), Determination of hydrocarbon prospective areas in the Tuzgolu (Saltlake) Basin, central Anatolia, by using geophysical data, *Journal of Pet. Sci. Eng.*, *62*, 36–44.

Barrier, E., and B. Vrielynck (2008), *MEBE Atlas of Paleotectonic Maps of the Middle East*, Commission for the Geological Map of the World, Paris.

Biryol, C. B., S. L. Beck, G. Zandt, and A. A. Özacar (2011), Segmented African lithosphere beneath the Anatolian region inferred from teleseismic *P*-wave tomography, *Geophys. J. Int.*, *184*, 1037–1057.

Boztuğ, D., and Y. Harlavan (2007), K–Ar ages of granitoids unravel the stages of Neo-Tethyan convergence in the eastern Pontides and central Anatolia, Turkey, *Int. J. Earth Sci.*, *97*, 585–599.

Boztuğ, D., and R. C. Jonckheere (2007), Apatite fission track data from central Anatolian granitoids (Turkey): Constraints on Neo-Tethyan closure, *Tectonics*, *26*, TC3011, doi:10.1029/2006TC001988.

Boztuğ, D., M. Tichomirowa, and K. Bombach (2007), ^{207}Pb–^{206}Pb single-zircon evaporation ages of some granitoid rocks reveal continent-oceanic island arc collision during the Cretaceous geodynamic evolution of the central Anatolian crust, Turkey, *J. Asian Earth Sci.*, *31*, 71–86.

Boztuğ, D., E. Turksever, M. Heizler, R. C. Jonckheere, and M. Tichomirowa (2009a), ^{207}Pb-^{206}Pb, ^{40}Ar-^{39}Ar and apatite fission-track geothermochronology revealing the emplacement, cooling and exhumation history of the Karacayır Syenite (N Sivas), East-Central Anatolia, Turkey, *Turk. J. Earth Sci.*, *18*, 109–125.

Boztuğ, D., Ö. Güney, M. Heizler, R. C. Jonckheere, M. Tichomirowa, and N. Otlu (2009b), ^{207}Pb-^{206}Pb, ^{40}Ar-^{39}Ar and fission-track geothermochronology quantifying cooling and exhumation history of the Kaman-Kırşehir region intrusions, central Anatolia, Turkey, *Turk. J. Earth Sci.*, *18*, 85–108.

Boztuğ, D., R. C. Jonckheere, M. Heizler, L. Ratschbacher, Y. Harlavan, and M. Tichomirova (2009c), Timing of post-obduction granitoids from intrusion through cooling to exhumation in central Anatolia, Turkey, *Tectonophysics*, *473*, 223–233.

Cakir, U., T. Juteau, and H. Whitechurch (1978), Nouvelles preuves de l'écaillage intra-océanique précoce des ophiolites téthysiennes: Les roches métamorphiques infra-péridotitiques du massif de Pozanti-Karsanti (Turquie), *Bull. Soc. Géol. Fr.*, *7*, 61–70.

Candan, O., M. Cetinkaplan, R. Oberhänsli, G. Rimmelé, and C. Akal (2005), Alpine high-P/low-T metamorphism of the Afyon Zone and implications for the metamorphic evolution of Western Anatolia, Turkey, *Lithos*, *84*, 102–124.

Candan, O., O. E. Koralay, G. Topuz, R. Oberhänsli, H. Fritz, A. S. Collins, and F. Chen (2015), Late Neoproterozoic gabbro emplacement followed by early Cambrian eclogite-facies metamorphism in the Menderes Massif (W. Turkey): Implications on the final assembly of Gondwana, *Gondwana Res.*, doi:10.1016/j.gr.2015.02.015, in press.

Casey, J. F., and J. F. Dewey (1984), Initiation of subduction zones along transform and accreting plate boundaries, triple-junction evolution, and forearc spreading centres—Implications for ophiolitic geology and obduction, *Geol. Soc. London, Spec. Publ.*, *13*, 269–290.

Cassata, W. S., and P. R. Renne (2013), Systematic variations of argon diffusion in feldspars and implications for thermochronometry, *Geochim. Cosmochim. Acta*, *112*, 251–287.

Çelik, Ö. F. (2007), Metamorphic sole rocks and their mafic dykes in the eastern Tauride belt ophiolites (southern Turkey): Implications for OIB-type magma generation following slab break-off, *Geol. Mag.*, *144*, 849–866.

Çelik, Ö. F. (2008), Detailed geochemistry and K-Ar geochronology of the metamorphic sole rocks and their mafic dykes from the Mersin Ophiolite, Southern Turkey, *Turk. J. Earth Sci.*, *17*, 685–708.

Çelik, Ö. F., and M. F. Delaloyle (2003), Origin of metamorphic soles and their post-kinematic mafic dyke swarms in the Antalya and Lycian ophiolites, SW Turkey, *Geol. J.*, *38*, 235–256.

Çelik, Ö. F., M. F. Delaloyle, and G. Feraud (2006), Precise ^{40}Ar–^{39}Ar ages from the metamorphic sole rocks of the Tauride Belt Ophiolites, southern Turkey: Implications for the rapid cooling history, *Geol. Mag.*, *143*, 213–227.

Çelik, Ö. F., A. Marzoli, R. Marschik, M. Chiaradia, F. Neubauer, and I. Öz (2011), Early–Middle Jurassic intra-oceanic subduction in the İzmir-Ankara-Erzincan Ocean, Northern Turkey, *Tectonophysics*, *509*, 120–134.

Çelik, Ö. F., M. Chiaradia, A. Marzoli, Z. Billor, and R. Marschik (2013), The Eldivan ophiolite and volcanic rocks in the İzmir–Ankara–Erzincan suture zone, Northern Turkey: Geochronology, whole-rock geochemical and Nd–Sr–Pb isotope characteristics, *Lithos*, *172–173*, 31–46.

Cemen, I., M. C. Göncüoglu, and K. Dirik (1999), Structural evolution of the Tuzgölü basin in Central Anatolia, Turkey, *J. Geol.*, *107*, 693–706.

Cetinkaplan, M., A. Pourteau, O. Candan, O. E. Koralay, R. Oberhänsli, A. I. Okay, F. Chen, H. Kozlu, and F. Şengün (2016), P–T–t evolution of eclogite/blueschist facies metamorphism in Alanya Massif: Time and space relations with HP event in Bitlis Massif, Turkey, *Int. J. Earth Sci.*, *105*, 247–281.

Chadima, M., and F. Hrouda (2006), Remasoft 3.0 a user-friendly paleomagnetic data 152 browser and analyzer, *Trav. Géophys.*, *27*, 20–21.

Clark, M., and A. H. F. Robertson (2002), The role of the Early Tertiary Ulukisla Basin, southern Turkey, in suturing of the Mesozoic Tethys ocean, *J. Geol. Soc.*, *159*, 673–690.

Corfu, F. (2004), U-Pb age, setting and tectonic significance of the anorthosite-mangerite-charnockite-Granite Suite, Lofoten-Vesteralen, Norway, *J. Petrol.*, *45*, 1799–1819.

Cox, A., and R. B. Hart (1986), *Plate Tectonics, How It Works*, John Wiley, Oxford, U. K.

Daşçı, H. T., O. Parlak, N. Nurlu, and Z. Billor (2014), Geochemical characteristics and age of metamorphic sole rocks within a Neotethyan ophiolitic mélange from Konya region (central southern Turkey), *Geodin. Acta*, 1–21.

Davis, P. B., and D. L. Whitney (2008), Petrogenesis and structural petrology of high-pressure metabasalt pods, Sivrihisar, Turkey, *Contrib. Mineral. Petrol.*, *156*, 217–241.

Deenen, M. H. L., C. G. Langereis, D. J. J. van Hinsbergen, and A. J. Biggin (2011), Geomagnetic secular variation and the statistics of palaeomagnetic directions, *Geophys. J. Int.*, *186*, 509–520.

Delibaş, O., and Y. Genç (2012a), Late Cretaceous coeval acidic and basic magmatism, Karacaali Magmatic Complex, Central Anatolia, Turkey, *Int. Geol. Rev.*, *54*, 1697–1720.

Delibaş, O., and Y. Genç (2012b), Re-Os molybdenite ages of granitoid-hosted Mo–Cu occurrences from central Anatolia (Turkey), *Ore Geol. Rev.*, *44*, 39–48.

Delibaş, O., Y. Genç, and C. P. De Campos (2011), Magma mixing and unmixing related mineralization in the Karacaali Magmatic Complex, central Anatolia, Turkey, *Geol. Soc. London, Spec. Publ.*, *350*, 149–173.

Dewey, J. F., and J. F. Casey (2013), The sole of an ophiolite: The Ordovician Bay of Islands Complex, Newfoundland, *J. Geol. Soc.*, *170*, 715–722.

Dewey, J. F., and A. M. C. Sengör (1979), Aegean and surrounding regions: Complex multiplate and continuum tectonics in a convergent zone, *Geol. Soc. Am. Bull.*, *90*, 84–92.

Dilek, Y., and H. Furnes (2011), Ophiolite genesis and global tectonics: Geochemical and tectonic fingerprinting of ancient oceanic lithosphere, *Geol. Soc. Am. Bull.*, *123*(3–4), 387–411.

Dilek, Y., and D. L. Whitney (1997), Counterclockwise P-T-t trajectory from the metamorphic sole of a Neo-Tethyan ophiolite (Turkey), *Tectonophysics*, *280*, 295–310.

Dilek, Y., P. Thy, B. R. Hacker, and S. Grundvig (1999), Structure and petrology of Tauride ophiolites and mafic dike intrusions (Turkey): Implications for the Neotethyan ocean, *Geol. Soc. Am. Bull.*, *111*, 1192–1216.

Dilek, Y., H. Furnes, and M. Shallo (2007), Suprasubduction zone ophiolite formation along the periphery of Mesozoic Gondwana, *Gondwana Res.*, *11*, 453–475.

Droop, G. T. R., M. Karakaya, Y. Eren, and N. Karakaya (2005), Metamorphic evolution of blueschists of the Altınekin Complex, Konya area, south central Turkey, *Geol. J.*, *40*, 127–153.

Dunlop, D., and Ö. Özdemir (1997), *Rock Magnetism: Fundamentals and Frontiers*, Cambridge Univ. Press, Cambridge.

Espurt, N., J. C. Hippolyte, N. Kaymakci, and E. Sangu (2014), Lithospheric structural control on inversion of the southern margin of the Black Sea Basin, Central Pontides, Turkey, *Lithosphere*, *6*, 26–34.

Faccenna, C., O. Bellier, J. Martinod, C. Piromallo, and V. Regard (2006), Slab detachment beneath eastern Anatolia: A possible cause for the formation of the North Anatolian fault, *Earth Planet. Sci. Lett.*, *242*, 85–97.

Faccenna, C., et al. (2014), Mantle dynamics in the Mediterranean, *Rev. Geophys.*, *52*, 283–332, doi:10.1002/2013RG000444.

Fayon, A. K., D. L. Whitney, C. Teyssier, J. I. Garver, and Y. Dilek (2001), Effects of plate convergence obliquity on timing and mechanisms of exhumation of a mid-crustal terrain, the Central Anatolian Crystalline Complex, *Earth Planet. Sci. Lett.*, *192*, 191–205.
Fernandez-Blanco, D., G. Bertotti, and T. A. Çiner (2013), Cenozoic tectonics of the Tuz Gölü Basin (Central Anatolia Plateau, Turkey), *Turk. J. Earth Sci.*, *22*, 715–738.
Fisher, R. A. (1953), Dispersion on a sphere, *Proc. R. Soc. London*, *A217*, 295–305.
Floyd, P. A., M. K. Yaliniz, and M. C. Göncüoğlu (1998), Geochemistry and petrogenesis of intrusive and extrusive ophiolitic plagiogranites, Central Anatolian Crystalline Complex, Turkey, *Lithos*, *42*, 225–241.
Floyd, P. A., M. C. Göncüoglu, J. A. Winchester, and K. M. Yalınız (2000), Geochemical character and tectonic environment of Neotethyan ophiolitic fragments and metabasites in the Central Anatolian Crystalline Complex, Turkey, in *Tectonics and Magmatism in Turkey and the Surrounding Area*, *Geol. Soc. Spec. Publ.*, vol. 173, edited by P. A. Floyd et al., pp. 183–202.
Frizon de Lamotte, D., C. Raulin, N. Mouchot, J.-C. Wrobel-Daveau, C. Blanpied, and J.-C. Ringenbach (2011), The southernmost margin of the Tethys realm during the Mesozoic and Cenozoic: Initial geometry and timing of the inversion processes, *Tectonics*, *30*, TC3002, doi:10.1029/2010TC002691.
Gaina, C., T. H. Torsvik, D. J. J. van Hinsbergen, S. Medvedev, S. C. Werner, and C. Labails (2013), The African Plate: A history of oceanic crust accretion and subduction since the Jurassic, *Tectonophysics*, *604*, 4–25.
Gautier, P., E. Bozkurt, E. Hallot, and K. Dirik (2002), Dating the exhumation of a metamorphic dome: Geological evidence for pre-Eocene unroofing of the Nigde Massif (Central Anatolia, Turkey), *Geol. Mag.*, *139*, 559–576.
Gautier, P., E. Bozkurt, V. Bosse, E. Hallot, and K. Dirik (2008), Coeval extensional shearing and lateral underflow during Late Cretaceous core complex development in the Niğde Massif, Central Anatolia, Turkey, *Tectonics*, *27*, TC1003–doi:10.1029/2006TC002089.
Gessner, K., A. S. Collins, U. Ring, and T. Güngör (2004), Structural and thermal history of poly-orogenic basement: U-Pb geochronology of granitoid rocks in the southern Menderes Massif, Western Turkey, *J. Geol. Soc.*, *161*, 93–101.
Gill, J. B. (1981), *Orogenic Andesites and Plate Tectonics*, Springer, New York.
Göncüoğlu, M. C. (1986), Geochronological data from the southern part (Niğde area) of the Central Anatolian Massif, *Miner. Res. Tech. Inst. Turk.*, *105*(106), 83–96.
Göncüoğlu, M. C., V. Toprak, I. Kuscu, A. Erler, and E. Olgun (1991), Geology of the western part of the Central Anatolian Massif, part 1: Southern section [in Turkish], Turkish Petroleum Corporation (TPAO) Rep., 2909, 1–140.
Görür, N., F. Y. Oktay, I. Seymen, and A. M. C. Sengör (1984), Palaeotectonic evolution of the Tuzgolu basin complex, Central Turkey: Sedimentary record of a Neo-Tethyan closure, *Geol. Soc. London, Spec. Publ.*, *17*, 467–482.
Grove, M., and T. M. Harrison (1996), ^{40}Ar* diffusion in Fe-rich biotite, *Am. Mineral.*, *81*, 940–951.
Güleç, N. (1994), Rb–Sr isotope data from the Ağaçören granitoid (east of Tuz Gölü): Geochronological and genetical implications, *Turk. J. Earth Sci.*, *3*, 39–43.
Gülyüz, E., N. Kaymakci, M. J. M. Meijers, D. J. J. van Hinsbergen, C. Lefebvre, R. L. M. Vissers, B. W. H. Hendriks, and A. A. Peynircioğlu (2013), Late Eocene evolution of the Çiçekdağı Basin (central Turkey): Syn-sedimentary compression during microcontinent–continent collision in central Anatolia, *Tectonophysics*, *602*, 286–299.
Hacker, B. R. (1990), Simulation of the metamorphic and deformational history of the metamorphic sole of the Oman ophiolite, *J. Geophys. Res.*, *95*, 4895–4907, doi:10.1029/JB095iB04p04895.
Hacker, B. R., and E. Gnos (1997), The conundrum of Samail: Explaining the metamorphic history, *Tectonophysics*, *279*, 215–226.
Handy, M. R., S. M. Schmid, R. Bousquet, E. Kissling, and D. Bernoulli (2010), Reconciling plate-tectonic reconstructions of Alpine Tethys with the geological–geophysical record of spreading and subduction in the Alps, *Earth Sci. Rev.*, *102*, 121–158.
Harrison, T. M. (1981), Diffusion of ^{40}Ar in hornblende, *Contrib. Mineral. Petrol.*, *78*, 324–331.
Harrison, T. M., and I. McDougall (1982), The thermal significance of potassium feldspar/k-Ar ages inferred from ^{40}Ar/^{39}Ar age spectrum results, *Geochim. Cosmochim. Acta*, *46*, 1811–1820.
Harrison, T. M., J. Célérier, A. B. Aikman, J. Hermann, and M. T. Heizler (2009), Diffusion of ^{40}Ar in muscovite, *Geochim. Cosmochim. Acta*, *73*, 1039–1051.
Hurst, S. D., K. L. Verosub, and E. M. Moores (1992), Paleomagnetic constraints on the formation of the Solea graben, Troodos ophiolite, Cyprus, *Tectonophysics*, *208*, 431–445.
Hüsing, S. K., W. J. Zachariasse, D. J. J. van Hinsbergen, W. Krijgsman, M. Inceoz, M. Harzhauser, O. Mandic, and A. Kroh (2009), Oligocene-Miocene basin evolution in SE Anatolia, Turkey: Constraints on the closure of the eastern Tethys gateway, *Geol. Soc. London, Spec. Publ.*, *311*, 107–132.
Idleman, L., M. A. Cosca, M. T. Heizler, S. N. Thomson, C. Teyssier, and D. L. Whitney (2014), Tectonic burial and exhumation cycles tracked by muscovite and K-feldspar ^{40}Ar/^{39}Ar thermochronology in a strike-slip fault zone, central Turkey, *Tectonophysics*, *612–613*, 134–146.
İlbeyli, N. (2004a), Petrogenesis of collision-related plutonics in Central Anatolia, Turkey, *Lithos*, *72*, 163–182.
İlbeyli, N. (2004b), Field, Petrographic and geochemical characteristics of the Hamit alkaline intrusion in the Central Anatolian Crystalline Complex, Turkey, *Turk. J. Earth Sci.*, *13*, 269–286.
İlbeyli, N. (2005), Mineralogical–geochemical constraints on intrusives in central Anatolia, Turkey: Tectono-magmatic evolution and characteristics of mantle source, *Geol. Mag.*, *142*, 187–207.
İlbeyli, N. (2008), Geochemical comparison of ultramafic-mafic cumulate rocks from the Central Anatolian ophiolites, Turkey, *Int. Geol. Rev.*, *50*, 810–825.
İlbeyli, N., J. A. Pearce, and I. G. Meighan (2009), Contemporaneous late Cretaceous calc-alkaline and alkaline magmatism in central Anatolia, Turkey: Oxygen isotope constraints on petrogenesis, *Turk. J. Earth Sci.*, *18*, 529–547.
Inwood, J., A. Morris, and M. W. Anderson (2009), Neotethyan intraoceanic microplate rotation and variations in spreading axis orientation: Palaeomagnetic evidence from the Hatay ophiolite (southern Turkey), *Earth Planet. Sci. Lett.*, *280*, 105–117.
Işık, V. (2009), The ductile shear zone in granitoid of the Central Anatolian Crystalline Complex, Turkey: Implications for the origins of the Tuzgölü basin during the Late Cretaceous extensional deformation, *J. Asian Earth Sci.*, *34*, 507–521.
Işık, V., C.-H. Lo, C. Göncüoğlu, and S. Demirel (2008), ^{39}Ar/^{40}Ar ages from the Yozgat Batholith: Preliminary data on the timing of Late Cretaceous extension in the Central Anatolian Crystalline Complex, Turkey, *J. Geol.*, *116*, 510–526.
Işık, V., I. T. Uysal, A. Caglayan, and G. Seyitoglu (2014), The evolution of intraplate fault systems in central Turkey: Structural evidence and Ar-Ar and Rb-Sr age constraints for the Savcili Fault Zone, *Tectonics*, *33*, 1875–1899, doi:10.1002/2014TC003565.
Jaffey, A., K. Flynn, L. Glendenin, W. Bentley, and A. Essling (1971), Precision measurement of half-lives and specific activities of ^{235}U and ^{238}U, *Phys. Rev. C*, *4*, 1889–1906.
Johnson, C. L., et al. (2008), Recent investigations of the 0–5 Ma geomagnetic field recorded by lava flows, *Geochem. Geophys. Geosyst.*, *9*, Q04032, doi:10.1029/2007GC001696.

Jolivet, L., C. Facenna, B. Goffé, E. Burov, and P. Agard (2003), Subduction tectonics and exhumation of high-pressure metamorphic rocks in the Mediterranean orogen, *Am. J. Sci.*, *303*, 353–409.
Jolivet, L., C. Faccenna, and C. Piromallo (2009), From mantle to crust: Stretching the Mediterranean, *Earth Planet. Sci. Lett.*, *285*, 198–209.
Kadıoğlu, Y. K., Y. Dilek, N. Gülec, and K. A. Foland (2003), Tectonomagmatic evolution of bimodal plutons in the Central Anatolian Crystalline Complex, Turkey, *J. Geol.*, *111*, 671–690.
Kadıoğlu, Y. K., Y. Dilek, and K. A. Foland (2006), Slab break-off and syncollisional origin of the Late Cretaceous magmatism in the Central Anatolian crystalline complex, Turkey, *Geol. Soc. Am. Spec. Pap.*, *409*, 381–415.
Kaymakci, N., C. E. Duermeijer, C. Langereis, S. H. White, and P. M. Van Dijk (2003), Palaeomagnetic evolution of the Çankırı Basin (central Anatolia, Turkey): Implications for oroclinal bending due to indentation, *Geol. Mag.*, *140*, 343–355.
Kaymakci, N., Y. Ozcelik, S. H. White, and P. M. Van Dijk (2009), Tectono-stratigraphy of the Cankiri Basin: Late Cretaceous to early Miocene evolution of the Neotethyan Suture Zone in Turkey, *Geol. Soc. London, Spec. Publ.*, *311*, 67–106.
Keskin, M. (2003), Magma generation by slab steepening and breakoff beneath a subduction-accretion complex: An alternative model for collision-related volcanism in Eastern Anatolia, Turkey, *Geophys. Res. Lett.*, *30*(24), 8046, doi:10.1029/2003GL018019.
Kimura, G. (1986), Oblique subduction and collision: Forearc tectonics of the Kuril arc, *Geology*, *14*, 404–407.
Kirker, A., and E. McClelland (1996), Application of net tectonic rotations and inclination analysis to a high-resolution palaeomagnetic study in the Betic Cordillera, *Spec. Publ. - Geol. Soc. London*, *105*, 19–32.
Kirschvink, J. L. (1980), The least-squares line and plane and the analysis of palaeomagnetic data, *Geophys. J. R. Astrol. Soc.*, *62*, 699–718.
Koç, A., N. Kaymakci, D. J. J. van Hinsbergen, K. F. Kuiper, and R. L. M. Vissers (2012), Tectono-Sedimentary evolution and geochronology of the Middle Miocene Altınapa Basin, and implications for the Late Cenozoic uplift history of the Taurides, southern Turkey, *Tectonophysics*, *532–535*, 134–155.
Koç, A., D. J. J. van Hinsbergen, C. G. Langereis, and N. Kaymakcı (2016a), Late Neogene oroclinal bending in the central Taurides: A record of termination of eastward subduction in southern Turkey?, *Earth Planet. Sci. Lett.*, *434*, 75–90.
Koç, A., N. Kaymakci, D. J. J. van Hinsbergen, and R. L. M. Vissers (2016b), A Miocene onset of the modern extensional regime in the Isparta Angle: Constraints from the Yalvaç Basin (southwest Turkey), *Int. J. Earth Sci.*, *105*, 369–398.
Kocyigit, A. (1991), An example of an accretionary forearc basin from northern Central Anatolia and its implications for the history of subduction of Neo-Tethys in Turkey, *Geol. Soc. Am. Bull.*, *103*, 22–36.
Köksal, S., and M. C. Göncüoglu (1997), Geology if the İdiş Dağı-Avanos area (Nevşehir-Central Anatolia), *Miner. Res. Explor. Bull.*, *119*, 41–58.
Köksal, S., R. L. Romer, M. C. Göncüoğlu, and F. Toksoy-Köksal (2004), Timing of post-collisional H-type to A-type granitic magmatism: U-Pb titanite ages from the Alpine central Anatolian granitoids (Turkey), *Int. J. Earth Sci.*, *93*, 974–989.
Köksal, S., A. Möller, M. C. Göncüoglu, D. Frei, and A. Gerdes (2012), Crustal homogenization revealed by U–Pb zircon ages and Hf isotope evidence from the Late Cretaceous granitoids of the Agaçören intrusive suite (Central Anatolia/Turkey), *Contrib. Mineral. Petrol.*, *163*, 725–743.
Köksal, S., F. Toksoy-Köksal, M. C. Göncüoglu, A. Möller, A. Gerdes, and D. Frei (2013), Crustal source of the Late Cretaceous Satansarı monzonite stock (central Anatolia – Turkey) and its significance for the Alpine geodynamic evolution, *J. Geodyn.*, *65*, 82–93.
Krogh, T. E. (1973), A low-contamination method for hydrothermal decomposition of zircon and extraction of U and Pb for isotopic age determinations, *Geochim. Cosmochim. Acta*, *37*, 485–494.
Krogh, T. E. (1982), Improved accuracy of U-Pb zircon dating by selection of more concordant fractions using a high gradient magnetic separation technique, *Geochim. Cosmochim. Acta*, *46*, 631–635.
Lázaro, C., A. García-Casco, Y. Rojas Agramonte, A. Kröner, F. Neubauer, and M. A. Iturralde-Vinent (2009), Fifty-five-million-year history of oceanic subduction and exhumation at the northern edge of the Caribbean plate (Sierra del Convento melange, Cuba), *J. Metamorph. Geol.*, *27*, 19–40.
Lefebvre, C. (2011), The tectonics of the Central Anatolian Crystalline Complex: A structural, metamorphic and paleomagnetic study, in *Utrecht Studies in Earth Sciences*, vol. 3, 147 pp., Utrecht Univ., Utrecht, Neth.
Lefebvre, C., A. Barnhoorn, D. J. J. van Hinsbergen, N. Kaymakci, and R. L. M. Vissers (2011), Late Cretaceous extensional denudation along a marble detachment fault zone in the Kırşehir massif near Kaman, central Turkey, *J. Struct. Geol.*, *33*, 1220–1236.
Lefebvre, C., M. J. M. Meijers, N. Kaymakci, A. Peynircioğlu, C. G. Langereis, and D. J. J. van Hinsbergen (2013), Reconstructing the geometry of central Anatolia during the late Cretaceous: Large-scale Cenozoic rotations and deformation between the Pontid es and Taurides, *Earth Planet. Sci. Lett.*, *366*, 83–98.
Lefebvre, C., K. Peters, P. Wehrens, F. M. Brouwer, and H. L. M. Van Roermund (2015), Thermal and extensional exhumation history of a high-temperature crystalline complex (Hırkadağ Massif, Central Anatolia), *Lithos*, *238*, 156–173.
Lisenbee, A. L. (1972), Structural Setting of the Orhaneli Ultramafic Massif Near Bursa, Northwestern Turkey, PhD thesis, Pennsylvania State Univ., 157 pp.
Ludwig, K. R. (2003), User's Manual for Isoplot 3.00, Berkeley Geochronology Center Special Publication.
Lytwyn, J. N., and J. F. Casey (1993), The geochemistry and petrogenesis of volcanics and sheeted dikes from the Hatay (Kizildag) ophiolite, southern Turkey: Possible formation with the Troodos ophiolite, Cyprus, along fore-arc spreading centers, *Tectonophysics*, *223*, 237–272.
Maffione, M., C. Thieulot, D. J. J. van Hinsbergen, A. Morris, O. Plumper, and W. Spakman (2015a), Dynamics of intraoceanic subduction initiation: 1. Oceanic detachment fault inversion and the formation of supra-subduction zone ophiolites, *Geochem. Geophys. Geosyst.*, *16*, 1753–1770, doi:10.1002/2015GC005746.
Maffione, M., D. J. J. van Hinsbergen, L. Koornneef, C. Guilmette, K. V. Hodges, N. Borneman, W. Huang, L. Ding, and P. Kapp (2015b), Forearc hyperextension dismembered the South Tibetan ophiolites, *Geology*, *43*, 475–478.
Mattinson, J. M. (2005), Zircon U–Pb chemical abrasion ("CA-TIMS") method: Combined annealing and multi-step partial dissolution analysis for improved precision and accuracy of zircon ages, *Chem. Geol.*, *220*, 47–66.
McDougall, I., and T. M. Harrison (1999), *Geochronology and Thermochronology by the 40Ar/39Ar Method*, Oxford Univ. Press, New York.
Meijers, M. J. M., N. Kaymakci, D. J. J. van Hinsbergen, C. G. Langereis, R. A. Stephenson, and J.-C. Hippolyte (2010), Late Cretaceous to Paleocene oroclinal bending in the central Pontides (Turkey), *Tectonics*, *29*, TC4016, doi:10.1029/2009TC002620.
Moix, P., L. Beccaletto, H. W. Kozur, C. Hochard, F. Rosselet, and G. M. Stampfli (2008), A new classification of the Turkish terranes and sutures and its implication for the paleotectonic history of the region, *Tectonophysics*, *451*, 7–39.
Monod, O. (1977), Récherches géologiques dans le Taurus occidental au sud de Beysehir (Turquie), Thèse Doctorat d'État, Univ. Paris-Sud, "Centre d"Orsay'.
Morris, A., K. M. Creer, and A. H. F. Robertson (1990), Palaeomagnetic evidence for clockwise rotations related to dextral shear along the Southern Troodos Transform Fault, Cyprus, *Earth Planet. Sci. Lett.*, *99*, 250–262.

Morris, A., M. W. Anderson, and A. H. F. Robertson (1998), Multiple tectonic rotations and transform tectonism in an intraoceanic suture zone, SW Cyprus, *Tectonophysics*, *299*, 229–253.
MTA (2002), Geological map of Turkey, 1:500,000, edited by M. Senel (1:500000).
Mulcahy, S. R., J. D. Vervoort, and P. R. Renne (2014), Dating subduction-zone metamorphism with combined garnet and lawsonite Lu-Hf geochronology, *J. Metamorph. Geol.*, *32*, 515–533.
Mullender, T., A. J. Van Velzen, and M. J. Dekkers (1993), Continuous drift correction and separate identification of ferrimagnetic and paramagnetic contributions in thermomagnetic runs, *Geophys. J. Int.*, *114*, 663–672.
Nicolas, A., G. Ceuleneer, F. Boudier, and M. Misseri (1988), Structural mapping in the Oman ophiolites: Mantle diapirism along an oceanic ridge, *Tectonophysics*, *151*, 27–56.
Nicolas, A., F. Boudier, B. Ildefonse, and E. Ball (2000), Accretion of Oman and United Arab Emirates ophiolite—Discussion of a new structural map, *Mar. Geophys. Res.*, *21*, 147–179.
Oberhänsli, R., O. Candan, Ö. O. Dora, and S. H. Dürr (1997), Eclogites within the Menderes Massif/Western Turkey, *Lithos*, *41*, 135–150.
Okay, A. I. (1980a), Lawsonite zone blueschists and a sodic amphibole producing reaction in the Tavşanli Region, Northwest Turkey, *Contrib. Mineral. Petrol.*, *75*, 179–186.
Okay, A. I. (1980b), Mineralogy, petrology, and phase relations of glaucophane-lawsonite zone blueschists from the Tavşanli Region, Northwest Turkey, *Contrib. Mineral. Petrol.*, *72*, 243–255.
Okay, A. I. (1982), Incipient blueschist metamorphism and metasomatism in the Tavşanli region, Northwest Turkey, *Contrib. Mineral. Petrol.*, *79*, 361–367.
Okay, A. I. (1984), *Distribution and Characteristics of the North-west Turkish Blueschists*, *Geol. Soc. Spec. Publ.*, vol. 17, edited by A. I. Okay, pp. 455–466.
Okay, A. I. (1986), High-pressure/low-temperature metamorphic rocks of Turkey, *Geol. Soc. Am. Mem.*, *164*, 333–347.
Okay, A. I. (2002), Jadeite-chloritoid-glaucophane-lawsonite blueschists in north-west Turkey: Unusually high P/T ratios in continental crust, *J. Metamorph. Geol.*, *20*, 757–768.
Okay, A. I., and S. P. Kelley (1994), Tectonic setting, petrology and geochronology of jadeite + glaucophane and chloritoid + glaucophane schists from north-west Turkey, *J. Metamorph. Geol.*, *12*, 455–466.
Okay, A. I., and A. M. Nikishin (2015), Tectonic evolution of the southern margin of Laurasia in the Black Sea region, *Int. Geol. Rev.*, *57*, 1051–1076.
Okay, A. I., and O. Tüysüz (1999), Tethyan sutures of northern Turkey, *Spec. Publ. - Geol. Soc. London*, *156*, 475–515.
Okay, A. I., and D. L. Whitney (2010), Blueschists, eclogites, ophiolites and suture zones in northwest Turkey: A review and a field excursion guide, *Ofioliti*, *35*, 131–172.
Okay, A. I., M. Satir, H. Maluski, M. Siyako, P. Monié, R. Metzger, and S. Akyüz (1996), 19 Paleo-and Neo-Tethyan events in northwestern Turkey: Geologic and geochronologic constraints, in *The Tectonic Evolution of Asia*, edited by A. Yin and T. M. Harrison, pp. 420–441, Cambridge Univ. Press, Cambridge, U. K.
Okay, A. I., N. B. W. Harris, and S. P. Kelley (1998), Exhumation of blueschists along a Tethyan suture in northwest Turkey, *Tectonophysics*, *285*, 275–299.
Okay, A. I., O. Tüysüz, M. Satir, S. Özkan-Altiner, D. Altiner, S. Sherlock, and R. H. Eren (2006), Cretaceous and Triassic subduction-accretion, high-pressure-low-temperature metamorphism, and continental growth in the Central Pontides, Turkey, *Geol. Soc. Am. Bull.*, *118*, 1247–1269.
Okay, A. I., M. Zattin, and W. Cavazza (2010), Apatite fission-track data for the Miocene Arabia-Eurasia collision, *Geology*, *38*, 35–38.
Okay, A. I., G. Sunal, S. Sherlock, D. Altıner, O. Tüysüz, A. R. C. Kylander-Clark, and M. Aygül (2013), Early Cretaceous sedimentation and orogeny on the active margin of Eurasia: Southern Central Pontides, Turkey, *Tectonics*, *32*, 1247–1271, doi:10.1002/tect.20077.
Önen, A. P. (2003), Neotethyan ophiolitic rocks of the Anatolides of NW Turkey and comparison with Tauride ophiolites, *J. Geol. Soc.*, *160*, 947–962.
Önen, A. P., and R. Hall (1993), Ophiolites and related metamorphic rocks from the Kütahya region, north-west Turkey, *Geol. J.*, *160*, 947–962.
Özbakır, A. D., A. M. C. Sengör, M. J. R. Wortel, and R. Govers (2013), The Pliny–Strabo trench region: A large shear zone resulting from slab tearing, *Earth Planet. Sci. Lett.*, *375*, 188–195.
Özdamar, Ş., M. F. Roden, F. Esenli, B. Uz, and J. M. Wampler (2012), Geochemical features and K-Ar age data from metadetrital rocks and high-K metasomatized metarhyolites in the Afyon- Bolkardağ Zone (Ilgin-Konya), SW Turkey, *Neues Jahrb. Mineral., Abh.*, *189*, 155–176.
Özdamar, Ş., M. Z. Billor, G. Sunal, F. Esenli, and M. F. Roden (2013), First U–Pb SHRIMP zircon and $^{40}Ar/^{39}Ar$ ages of metarhyolites from the Afyon–Bolkardag Zone, SW Turkey: Implications for the rifting and closure of the Neo-Tethys, *Gondwana Res.*, *24*, 377–391.
Özgül, N. (1984), Stratigraphy and tectonic evolution of the Central Taurides, in *Geology of the Taurus Belt. Proceedings of the International Tauride Symposium*, edited by O. Tekeli and M. C. Göncüoğlu, pp. 77–90, Cambridge, U. K.
Parlak, O. (2000), Geochemistry and significance of mafic dyke swarms in the Pozantı-Karsantı ophiolite (southern Turkey), *Turk. J. Earth Sci.*, *9*, 29–38.
Parlak, O., and M. Delaloyle (1996), Geochemistry and timing of post-metamorphic dyke emplacement in the Mersin Ophiolite (southern Turkey): New age constraints from $^{40}Ar/^{39}Ar$ geochronology, *Terra Nova*, *8*, 585–592.
Parlak, O., and M. Delaloye (1999), Precise $^{40}Ar/^{39}Ar$ ages from the metamorphic sole of the Mersin ophiolite (southern Turkey), *Tectonophysics*, *301*, 145–158.
Parlak, O., V. Höck, and M. Delaloye (2002), The supra-subduction zone Pozanti–Karsanti ophiolite, southern Turkey: Evidence for high-pressure crystal fractionation of ultramafic cumulates, *Lithos*, *65*, 205–224.
Parlak, O., H. Yilmaz, and D. Boztuğ (2006), Origin and tectonic significance of the metamorphic sole and isolated dykes of the Divrigi ophiolite (Sivas, Turkey): Evidence for slab break-off prior to ophiolite emplacement, *Turk. J. Earth Sci.*, *15*, 25–45.
Parlak, O., F. Karaoğlan, T. Rızaoğlu, U. Klötzli, F. Koller, and Z. Billor (2013), U–Pb and $^{40}Ar–^{39}Ar$ geochronology of the ophiolites and granitoids from the Tauride belt: Implications for the evolution of the Inner Tauride suture, *J. Geodyn.*, *65*, 22–37.
Pearce, J. A., S. J. Lippard, and S. Roberts (1984), Characteristics and tectonic significance of supra-subduction zone ophiolites, *Spec. Publ. - Geol. Soc. London*, *16*, 77–94.
Plunder, A., P. Agard, C. Chopin, and A. I. Okay (2013), Geodynamics of the Tavşanlı zone, western Turkey: Insights into subduction/obduction processes, *Tectonophysics*, *608*, 884–903.
Plunder, A., P. Agard, C. Chopin, A. Pourteau, and A. I. Okay (2015), Accretion, underplating and exhumation along a subduction interface: From subduction initiation to continental subduction (Tavşanlı zone, W. Turkey), *Lithos*, 1–89.
Pourteau, A., O. Candan, and R. Oberhänsli (2010), High-pressure metasediments in central Turkey: Constraints on the Neotethyan closure history, *Tectonics*, *29*, TC5004, doi:10.1029/2009TC002650.

Pourteau, A., M. Sudo, O. Candan, P. Lanari, O. Vidal, and R. Oberhänsli (2013), Neotethys closure history of Anatolia: Insights from ^{40}Ar-^{39}Ar geochronology and P-T estimation in high-pressure metasedimentary rocks, *J. Metamorph. Geol.*, *31*, 585–606.
Pourteau, A., R. Bousquet, O. Vidal, A. Plunder, E. Duesterhoeft, O. Candan, and R. Oberhänsli (2014), Multistage growth of Fe–Mg–carpholite and Fe–Mg–chloritoid, from field evidence to thermodynamic modelling, *Contrib. Mineral. Petrol.*, *168*, 1090–26.
Reilinger, R., S. McClusky, D. Paradissis, and S. Ergintav (2010), Geodetic constraints on the tectonic evolution of the Aegean region and strain accumulation along the Hellenic subduction zone, *Tectonophysics*, *488*, 22–30.
Rimmelé, G., L. Jolivet, R. Oberhänsli, and B. Goffé (2003), Deformation history of the high-pressure Lycian Nappes and implications for the tectonic evolution of SW Turkey, *Tectonics*, *22*(2), 1007, doi:10.1029/2001TC901041.
Robertson, A. (2004), Development of concepts concerning the genesis and emplacement of Tethyan ophiolites in the Eastern Mediterranean and Oman regions, *Earth Sci. Rev.*, *66*, 331–387.
Robertson, A. H. F. (2002), Overview of the genesis and emplacement of Mesozoic ophiolites in the Eastern Mediterranean Tethyan region, *Lithos*, *65*, 1–67.
Robertson, A. H. F., O. Parlak, and T. Ustaömer (2009), Melange genesis and ophiolite emplacement related to subduction of the northern margin of the Tauride-Anatolide continent, central and western Turkey, *Geol. Soc. London, Spec. Publ.*, *311*, 9–66.
Rosenbaum, G., and G. S. Lister (2004), Formation of arcuate orogenic belts in the western Mediterranean region, *Geol. Soc. Am. Spec. Pap.*, *383*, 41–56.
Şahin, M. B., and Y. Erkan (1999), The index minerals and mineral assemblages determined in metamorphites of Evciler-Çatköy (Çayiralan-Yozkat) segment of Akdağmadeni massif, *Miner. Res. Explor. Bull.*, *121*, 83–100.
Schärer, U. (1984), The effect of initial 230 Th disequilibrium on young U Pb ages: The Makalu case, Himalaya, *Earth Planet. Sci. Lett.*, *67*, 191–204.
Scott, D. J., and M. R. St-Onge (1995), Constraints on Pb closure temperature in titanite based on rocks from the Ungava orogen, Canada: Implications for U-Pb geochronology and P-T-t path determinations, *Geology*, *23*, 1123–1126.
Seaton, N. C. A., D. L. Whitney, C. Teyssier, E. Toraman, and M. T. Heizler (2009), Recrystallization of high-pressure marble (Sivrihisar, Turkey), *Tectonophysics*, *479*, 241–253.
Seaton, N. C. A., C. Teyssier, D. L. Whitney, and M. T. Heizler (2014), Quartz and calcite microfabric transitions in a pressure and temperature gradient, Sivrihisar, Turkey, *Geodin. Acta*, *26*, 191–206.
Sengör, A. M. C., and W. S. F. Kidd (1979), Post-collisional tectonics of the Turkish-Iranian plateau and a comparison with Tibet, *Tectonophysics*, *55*, 361–376.
Sengör, A. M. C., and Y. Yilmaz (1981), Tethyan evolution of Turkey: A plate tectonic approach, *Tectonophysics*, *75*, 181–241.
Sengör, A. M. C., S. Özeren, T. Genç, and E. Zor (2003), East Anatolian high plateau as a mantle-supported, north-south shortened domal structure, *Geophys. Res. Lett.*, *30*(24), 8045, doi:10.1029/2003GL017858.
Seton, M., et al. (2012), Global continental and ocean basin reconstructions since 200 Ma, *Earth Sci. Rev.*, *113*, 212–270.
Seymen, I. (1983), Tectonic features of Kaman group in comparison with those of its neighbouring formations around Tamadag (Kaman-Kırs ehir), *Bull. Geol. Soc. Turk.*, *26*, 89–98.
Sherlock, S., and S. Kelley (2002), Excess argon evolution in HP–LT rocks: A UVLAMP study of phengite and K-free minerals, NW Turkey, *Chem. Geol.*, *182*, 619–636.
Sherlock, S., S. Kelley, S. Inger, N. Harris, and A. I. Okay (1999), ^{40}Ar/^{39}Ar and Rb-Sr geochronology of high-pressure metamorphism and exhumation history of the Tavsanli Zone, NW Turkey, *Contrib. Mineral. Petrol.*, *137*, 46–58.
Shin, T. A., E. J. Catlos, L. Jacob, and K. Black (2013), Relationships between very high pressure subduction complex assemblages and intrusive granitoids in the Tavşanlı Zone, Sivrihisar Massif, central Anatolia, *Tectonophysics*, *595–596*, 183–197.
Stacey, J. S., and J. D. Kramers (1975), Approximation of terrestrial lead isotope evolution by a two-stage model, *Earth Planet. Sci. Lett.*, *26*(2), 207–221, doi:10.1016/0012-821X(75)90088-6.
Stern, R. J., and S. H. Bloomer (1992), Subduction zone infancy: Examples from the Eocene Izu-Bonin-Mariana and Jurassic California arcs, *Geol. Soc. Am. Bull.*, *104*, 1621–1636.
Stern, R. J., M. Reagan, O. Ishizuka, Y. Ohara, and S. A. Whattam (2012), To understand subduction initiation, study forearc crust: To understand forearc crust, study ophiolites, *Lithosphere*, *4*, 469–483.
Sternai, P., L. Jolivet, A. Menant, and T. Gerya (2014), Driving the upper plate surface deformation by slab rollback and mantle flow, *Earth Planet. Sci. Lett.*, *405*, 110–118.
Tatar, S., and D. Boztuğ (2005), The syn-collisional Danacıobası biotite leucogranite derived from the crustal thickening in central Anatolia (Kırıkkale), Turkey, *Geol. J.*, *40*, 571–591.
Tauxe, L., and G. S. Watson (1994), The fold test: An eigen analysis approach, *Earth Planet. Sci. Lett.*, *122*, 331–341.
Tekin, U. K., and M. C. Göncüoğlu (2007), Discovery of the oldest (Upper Ladinian to Middle Carnian) radiolarian assemblages from the Bornova Flysch zone in Western Turkey: Implications for the Neotethyan Izmir-Ankara ocean, *Ofioliti*, *32*, 131–150.
Tekin, U. K., M. C. Göncüoglu, and N. Turhan (2002), First evidence of Late Carnian radiolarians from the Izmir–Ankara suture complex, central Sakarya, Turkey: Implications for the opening age of the Izmir–Ankara branch of Neo-Tethys, *Geobios*, *35*, 127–135.
Toksoy-Köksal, F., and M. C. Göncüoğlu (2001), Petrology of the Kurancali phlogopitic metagabbro: An island arc-type ophiolitic sliver in the Central Anatolian Crystalline Complex, *Int. Geol. Rev.*, *43*, 624–639.
Toksoy-Köksal, F., M. C. Göncüoglu, and M. K. Yalınız (2001), Petrology of the Kurancali phlogopitic metagabbro: An island arc-type ophiolitic sliver in the Central Anatolian Crystalline Complex, *Int. Geol. Rev.*, *43*, 624–639.
Topuz, G., G. Göçmengil, Y. Rolland, Ö. F. Çelik, T. Zack, and A. K. Schmitt (2013), Jurassic accretionary complex and ophiolite from northeast Turkey: No evidence for the Cimmerian continental ribbon, *Geology*, *41*, 255–258.
Torsvik, T. H., et al. (2012), Phanerozoic polar wander, palaeogeography and dynamics, *Earth Sci. Rev.*, *114*, 325–368.
Umhoefer, P. J., D. L. Whitney, C. Teyssier, A. K. Fayon, G. Casale, and M. T. Heizler (2007), Yo-yo tectonics in a wrench zone, Central Anatolian fault zone, Turkey, *Geol. Soc. Am. Spec. Pap.*, *434*, 35–57.
van der Kaaden, G. (1966), The significance and distribution of glaucophane rocks in Turkey, *Bull. Miner. Res. Explor. Inst.*, *67*, 37–67.
van Hinsbergen, D. J. J., and S. M. Schmid (2012), Map view restoration of Aegean-West Anatolian accretion and extension since the Eocene, *Tectonics*, *31*, TC5005, doi:10.1029/2012TC003132.
van Hinsbergen, D. J. J., E. Hafkenscheid, W. Spakman, J. E. Meulenkamp, and M. J. R. Wortel (2005), Nappe stacking resulting from subduction of oceanic and continental lithosphere below Greece, *Geology*, *33*, 325–328.
van Hinsbergen, D. J. J., N. Kaymakci, W. Spakman, and T. H. Torsvik (2010), Reconciling the geological history of western Turkey with plate circuits and mantle tomography, *Earth Planet. Sci. Lett.*, *297*, 674–686.
van Hinsbergen, D. J. J., R. Vissers, and W. Spakman (2014), Origin and consequences of western Mediterranean subduction, rollback, and slab segmentation, *Tectonics*, *33*, 393–419, doi:10.1002/2013TC003349.

van Hinsbergen, D. J. J., et al. (2015), Dynamics of intraoceanic subduction initiation: 2. Suprasubduction zone ophiolite formation and metamorphic sole exhumation in context of absolute plate motions, *Geochem. Geophys. Geosyst.*, *16*, 1771–1785, doi:10.1002/2015GC005745.

Vissers, R., D. van Hinsbergen, P. T. Meijer, and G. B. Piccardo (2013), Kinematics of Jurassic ultra-slow spreading in the Piemonte Ligurian ocean, *Earth Planet. Sci. Lett.*, *380*, 138–150.

Whitney, D. L., and Y. Dilek (1998), Metamorphism during Alpine crustal thickening and extension in Central Anatolia, Turkey: The Nigde metamorphic core complex, *J. Petrol.*, *39*, 1385–1403.

Whitney, D. L., and Y. Dilek (2000), Andalusite–sillimanite–quartz veins as indicators of low-pressure–high-temperature deformation during late-stage unroofing of a metamorphic core complex, Turkey, *J. Metamorph. Geol.*, *18*, 59–66.

Whitney, D. L., and Y. Dilek (2001), Metamorphic and tectonic evolution of the Hirkidag Block, Central Anatolian Crystalline Complex, *Turk. J. Earth Sci.*, *10*, 1–15.

Whitney, D. L., and M. A. Hamilton (2004), Timing of high-grade metamorphism in central Turkey and the assembly of Anatolia, *J. Geol. Soc.*, *161*, 823–828.

Whitney, D. L., C. Teyssier, Y. Dilek, and A. K. Fayon (2001), Metamorphism of the Central Anatolian Crystalline Complex, Turkey: Influence of orogen-normal collision vs. wrench-dominated tectonics on P–T–t paths, *J. Metamorph. Geol.*, *19*(4), 411–432.

Whitney, D. L., C. Teyssier, A. K. Fayon, M. A. Hamilton, and M. Heizler (2003), Tectonic controls on metamorphism, partial melting, and intrusion: Timing and duration of regional metamorphism and magmatism in the Niğde Massif, Turkey, *Tectonophysics*, *376*, 37–60.

Whitney, D. L., C. Teyssier, and M. T. Heizler (2007), Gneiss domes, metamorphic core complexes, and wrench zones: Thermal and structural evolution of the Niğde Massif, central Anatolia, *Tectonics*, *26*, TC5002, doi:10.1029/2006TC002040.

Whitney, D. L., P. J. Umhoefer, C. Teyssier, and A. K. Fayon (2008), Yo-yo tectonics of the Nigde Massif during wrenching in Central Anatolia, *Turk. J. Earth Sci.*, *17*, 209–217.

Whitney, D. L., C. Teyssier, E. Toraman, N. C. A. Seaton, and A. K. Fayon (2010), Metamorphic and tectonic evolution of a structurally continuous blueschist-to-Barrovian terrane, Sivrihisar Massif, Turkey, *J. Metamorph. Geol.*, *29*, 193–212.

Yalınız, K. M., and M. C. Göncüoğlu (1998), General geological characteristics and distribution of the Central Anatolian Ophiolites, *Yerbilimleri*, *20*, 19–30.

Yalınız, K. M., and M. C. Güncüoglu (1999), Clinopyroxene compositions of the isotropic gabbros from the Sar›karaman ophiolite: New evidence on supra-subduction zone type magma genesis in Central Anatolia, *Turk. J. Earth Sci.*, *8*, 103–111.

Yalınız, K. M., N. S. Aydin, M. Lu, and O. Parlak (1999), Terlemez quartz monzonite of Central Anatolia (AksarayąSarõkaraman): Age, petrogenesis and geotectonic implications for ophiolite emplacement, *Geol. J.*, *34*, 233–242.

Yalınız, K. M., P. A. Floyd, and C. M. Göncüoglu (2000a), *Geochemistry of Volcanic Rocks from the Cicekdag, Ophiolite, Central Anatolia, Turkey, and their Inferred Tectonic Setting within the Northern Branch of the Neotethyan Ocean*, edited by K. M. Yalınız, P. A. Floyd, and C. M. Göncüoglu, *Geol. Soc. London Spec. Publ.*, *173*, 203–218.

Yaliniz, M., P. A. Floyd, and M. C. Göncüoğlu (1996), Supra-subduction zone ophiolites of Central Anatolia: Geochemical evidence from the Sarikaraman ophiolite, Aksaray, Turkey, *Mineral. Mag.*, *60*, 697–710.

Yalınız, M. K. (2008), A geochemical attempt to distinguish forearc and back arc ophiolites from the "supra-subuduction" Central Anatolian ophiolites (Turkey) by comparison with modern oceanic analogues, *Ofioliti*, *33*, 119–129.

Yalınız, M. K., M. C. Göncüoglu, and S. N. Oezkan-Altiner (2000b), Formation and emplacement ages of the SSZ-type Neotethyan ophiolites in Central Anatolia, Turkey: Palaeotectonic implications, *Geol. J.*, *35*, 53–68.

Yalınız, M. K., P. A. Floyd, and M. C. Göncüoglu (2000c), Petrology and geotectonic significance of plagiogranite from the Sarikaraman ophiolite (Central Anatolia, Turkey), *Ofioliti*, *25*, 31–37.

Yürür, M. T., and Y. Genç (2006), The Savcili thrust fault (Kirsehir region, central Anatolia): A backthrust fault, a suture zone or a secondary fracture in an extensional regime?, *Geol. Carpathica*, *57*, 47–56.

Zeck, H. P., and T. Ünlü (1988), Alpine ophiolite obduction before 110 ± 5 Ma ago, Taurus belt, eastern central Turkey, *Tectonophysics*, *145*, 55–62.

Zijderveld, J. D. A. (1967), A. C. demagnetization of rocks: Analysis of results, in *Methods in Palaeomagnetism*, edited by D. W. Collinson, K. M. Creer, and S. K. Runcorn, pp. 254–286, Elsevier, Amsterdam.